AD-A141 015 UNITED STATES AIR FORCE ACADEMY DEPARTMENT OF CHEMISTRY 1/2
RESEARCH: AY 1982-83(U) AIR FORCE ACADEMY CO
L P DAVIS ET AL. MAR 84 USAFA-TR-84-6

UNCLASSIFIED F/G 7/4 NL

2

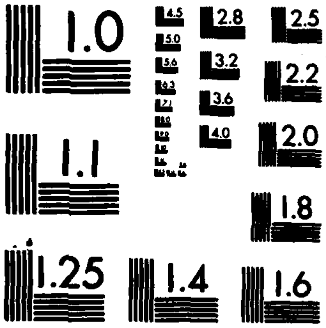

MICROCOPY RESOLUTION TEST CHART
NATIONAL BUREAU OF STANDARDS-1963-A

(12)

USAFA-TR-84-6

AD-A141 015

UNITED STATES AIR FORCE ACADEMY

DEPARTMENT OF CHEMISTRY RESEARCH:

AY 1982 - 83

MARCH 1984

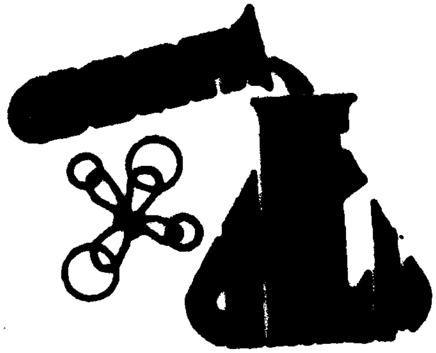

APPROVED FOR PUBLIC RELEASE; DISTRIBUTION UNLIMITED

DEAN OF THE FACULTY
UNITED STATES AIR FORCE ACADEMY
COLORADO SPRINGS, CO 80840

DTIC
MAY 11 1984
A

DTIC FILE COPY

84 05 10 038

This research report is presented as a competent treatment of the subject, worthy of publication. The United States Air Force Academy vouches for the quality of the research, without necessarily endorsing the opinions and conclusions of the author.

This report has been cleared for open publication and/or public release by the appropriate Office of Information in accordance with AFR 190-1 and AFR 12-30. There is no objection to unlimited distribution of this report to the public at large, or by DDC to the National Technical Information Service.

This research report has been reviewed and is approved for publication.

Thomas E McCann

THOMAS E. McCANN, Lt Col, USAF
Director of Research, Studies,
and Analysis

REPORT DOCUMENTATION PAGE

1a. REPORT SECURITY CLASSIFICATION UNCLASSIFIED

1b. RESTRICTIVE MARKINGS

2a. SECURITY CLASSIFICATION AUTHORITY

2b. DECLASSIFICATION/DOWNGRADING SCHEDULE

3. DISTRIBUTION/AVAILABILITY OF REPORT

4. PERFORMING ORGANIZATION REPORT NUMBER(S) USAFA-TR-84-6

5. MONITORING ORGANIZATION REPORT NUMBER(S)

6a. NAME OF PERFORMING ORGANIZATION
Department of Chemistry
Dean of the Faculty

6b. OFFICE SYMBOL *(If applicable)* USAFA/DFC

7a. NAME OF MONITORING ORGANIZATION

6c. ADDRESS *(City, State and ZIP Code)*
U.S. Air Force Academy
Colorado Springs, CO 80840

7b. ADDRESS *(City, State and ZIP Code)*

8a. NAME OF FUNDING/SPONSORING ORGANIZATION Frank J. Seiler Research Lab

8b. OFFICE SYMBOL *(If applicable)*

9. PROCUREMENT INSTRUMENT IDENTIFICATION NUMBER

8c. ADDRESS *(City, State and ZIP Code)*
United States Air Force Academy
Colorado Springs, CO 80840

10. SOURCE OF FUNDING NOS.

PROGRAM ELEMENT NO.	PROJECT NO.	TASK NO.	WORK UNIT NO.

11. TITLE *(Include Security Classification)* United States Air Force Academy Department of Chemistry Research: AY 1982-83 (U)

12. PERSONAL AUTHOR(S) Davis, Larry P., Major, Editor

13a. TYPE OF REPORT Final

13b. TIME COVERED FROM 1Jun82 TO 31May83

14. DATE OF REPORT *(Yr., Mo., Day)* 84 Mar

15. PAGE COUNT

16. SUPPLEMENTARY NOTATION

17. COSATI CODES

FIELD	GROUP	SUB. GR.
07	02	Inorganic Chem
07	03	Organic Chem
07	04	Physical Chem

18. SUBJECT TERMS *(Continue on reverse if necessary and identify by block number)* Chemical Research, Energetic Materials, Catalysis, Inorganic Chemistry, Biochemistry, Theoretical Chemistry

19. ABSTRACT *(Continue on reverse if necessary and identify by block number)*

Department of Chemistry research during AY 1982-83 has progressed well in the areas of energetic materials, theoretical chemistry, polymers for laser damage testing, and catalysts. Working closely with Frank J. Seiler Research Laboratory on many of these projects, department researchers have synthesized polymers for laser testing and new energetic compounds and have proposed new reaction mechanisms for the decomposition of explosives. Several analytical techniques and theoretical methods have been used to study catalyst surfaces. Several faculty have worked with cadets on independent research projects in the areas of inorganic synthesis, pigments from fungi, and preparation of new compounds.

20. DISTRIBUTION/AVAILABILITY OF ABSTRACT
UNCLASSIFIED/UNLIMITED ☒ SAME AS RPT. ☒ DTIC USERS ☐

21. ABSTRACT SECURITY CLASSIFICATION UNCLASSIFIED

22a. NAME OF RESPONSIBLE INDIVIDUAL Major Larry P. Davis

22b. TELEPHONE NUMBER *(Include Area Code)* (303) 472-2681

22c. OFFICE SYMBOL HQ USAFA/DFC

UNITED STATES AIR FORCE ACADEMY

Department of Chemistry Research:

AY 1982-83

Walter B. Avila
Silvia A. Beatty
Larry W. Burggraf
Larry P. Davis
Kenneth M. Dieter
Ronald O. Klatt
Hans J. Mueh
H. LeRoy Nyquist
Alan A. Shaffer
Henry H. Shin
Eric T. Smith
Almon G. Turner
Paul E. Vorndam
James R. Wright

Compiled and Edited
by
Larry P. Davis

March 1984

Preface

This technical report outlines the Department of Chemistry research efforts for academic year 1982-83. Each chapter covers specific accomplishments of one particular research product. We hope that it will be the first of an annual department technical report. It was compiled and edited by Major Larry P. Davis, the DFC Director of Research. Authors would like to thank Mrs. Pat Ridley for the expert typing.

Abstract

Department of Chemistry research during AY 1982-83 has progressed well in the areas of energetic materials, theoretical chemistry, polymers for laser damage testing, and catalysis. Working closely with the Frank J. Seiler Research Laboratory on many of these projects, department researchers have synthesized polymers for laser testing and new energetic compounds and have proposed new reaction mechanisms for the decomposition of explosives. Several analytical techniques and theoretical methods have been used to study catalyst surfaces. Several faculty have worked with cadets on independent research projects in the areas of inorganic synthesis, pigments from fungi, and preparation of new compounds.

TABLE OF CONTENTS

CHAPTER 1

REGIOSPECIFIC FLUORINATION OF ARYL ANIONS WITH XENON DIFLUORIDE

by Walter B. Avila, H. LeRoy Nyquist, and Eric T. Smith.

ABSTRACT

The reaction of xenon difluoride with organometallics is under investigation in an effort to develop a new synthesis of fluoroaromatics. Initial investigations involve a broad spectrum of organometallics with emphasis placed on organolithium and organomagnesium compounds. Initial results for the reaction of xenon difluorides reaction with phenylithium has given 16% fluorobenzene (relative to benzene by GC/mass spectral analysis). The effects of catalysts and chelating agents on product distribution as well as time, temperature, solvent studies are being investigated in order to optimize the reaction conditions.

INTRODUCTION

Aromatic fluorine containing compounds play an important role in several areas of chemistry. Fluorobenzoic acids have considerable potential in aromatic nucleophilic substitution and are useful reagents for the preparation of unsymmetrically substituted biaryls and benzoic acids.[1] Fluorine containing tranquilizers (I),[2] antibiotics (II),[3] and analgesic-antiinflammatory (III)[4] compounds, are just a few of the agents of interest in medicinal chemistry. Other fluorine containing aromatics are of interest in studies of chemical carcinogenesis.[5] In the area of energetic materials the incorporation of fluorine into compounds imparts thermal stability as well as enhancing the energy output of these materials. We are specifically interested in developing synthetic methodology for the regiospecific fluorination of aromatic compounds. While this methodology would be useful in each of the above areas, our main emphasis is directed toward the preparation of energetic materials for potential use as polymers and explosives in new weapon systems.

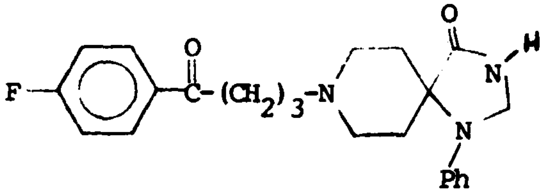

Spiropiperone I

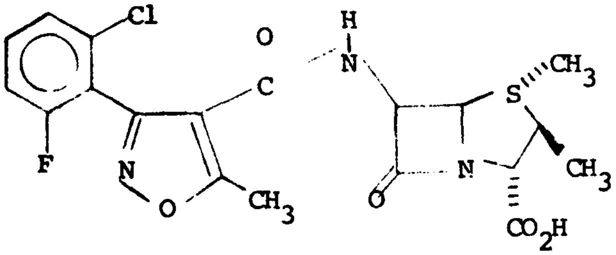

Floxacillin II

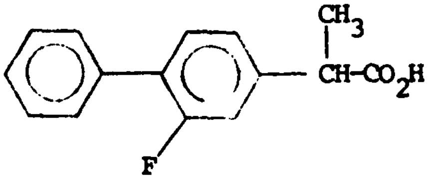

Flubiprofen III

The history of fluorinating organic compounds dates back to the discovery of fluorine in 1886 by M.H. Moissan. During the next several decades, little was done with this unusual molecule due to its difficult preparation and extreme reactivity. It was not until World War II and the initiation of the Manhattan Project that the impetus was provided for the development of fluorine chemistry. With this development came the discovery that fluorine containing materials possessed special and unusual properties. Besides unusual physical properties it was also determined that incorporation of a fluorine nucleus into bioactive molecules often increased their activity significantly. Fluorine containing compounds of all types were prepared and studied. The most difficult class to prepare was the aromatic fluorinated compounds.

The preparation of aromatic monofluorinated compounds suffers several disadvantages. First, several of the conventional fluorinating reagents are ineffective in producing fluorinated aromatics. They are extremely reactive and usually produce a wide range of products, none being the monofluorinated analogs. Secondly, many of the reactions are non-regiospecific. Finally, the fluorinating procedures require the handling of toxic or explosive materials which require specialized equipment. Our work is directed toward developmenting a regiospecific fluorination of aryl compounds that is compatible with a variety of functional groups and is easily carried out using standard laboratory equipment.

BACKGROUND

Fluorination of aromatic compounds with elemental fluorine,[6] hydrofluoric acid,[7] or high valency metal fluorides[8] is essentially ineffective. With few exceptions the reaction products are complex mixtures containing no aromatic fluorocompounds. Introduction of fluorine into the aromatic nucleus may be accomplished, however, by the Schiemann reaction[9] (Equation 1). The Schiemann reaction has been used to prepare a wide variety of fluorine containing aromatics. It does have several limitations[10] and groups which increase the solubility of the diazonium ion or promote side reactions during the decomposition stage lower the overall yield significantly. Also the preparation of amines is usually a multi-step process. An equally successful, if somewhat limited, synthesis of fluoroaromatics involves the displacement of activated halogens on an aromatic

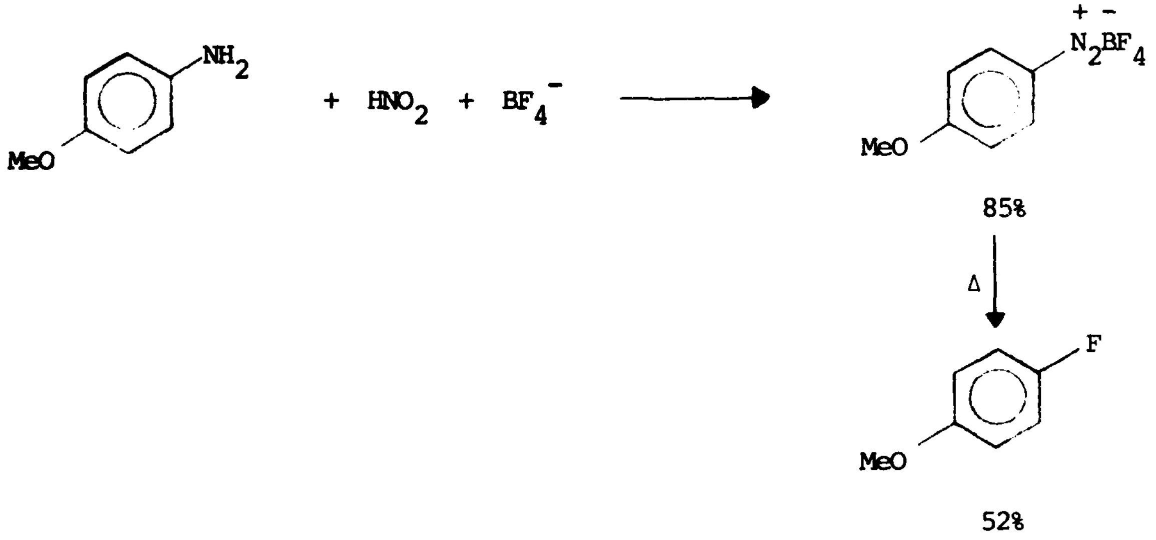

(1)

ring[11] (Equation 2).

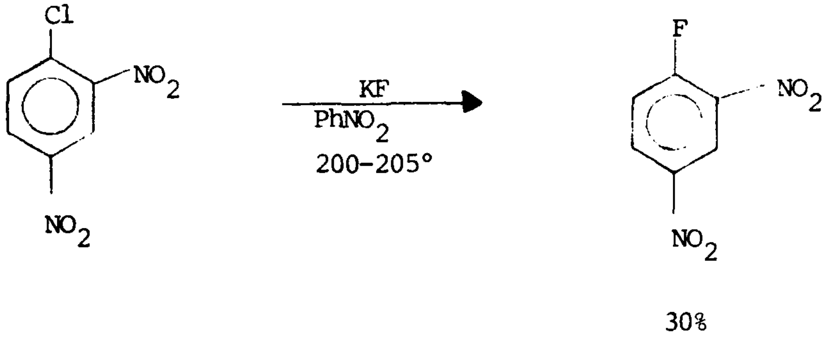

(2)

Parafluoroaminoaromatics have been prepared[12] in moderate yields as shown in Equation 3 and Taylor[13] and coworkers have used arylthallium compounds to obtain fluoroaromatics (Equation 4).

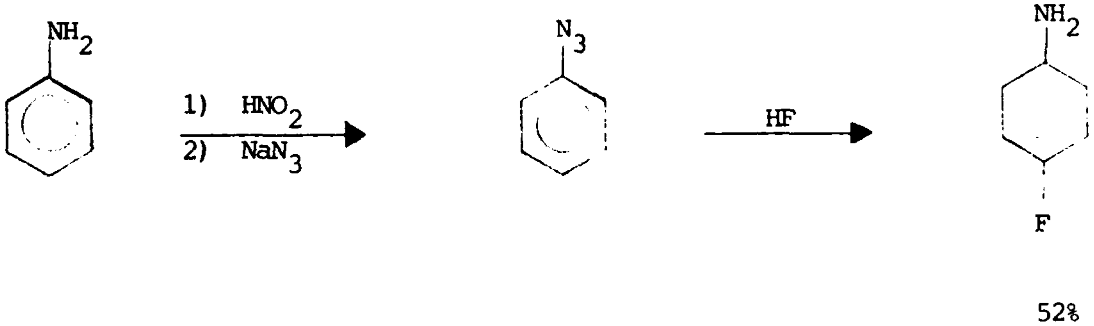

(3)

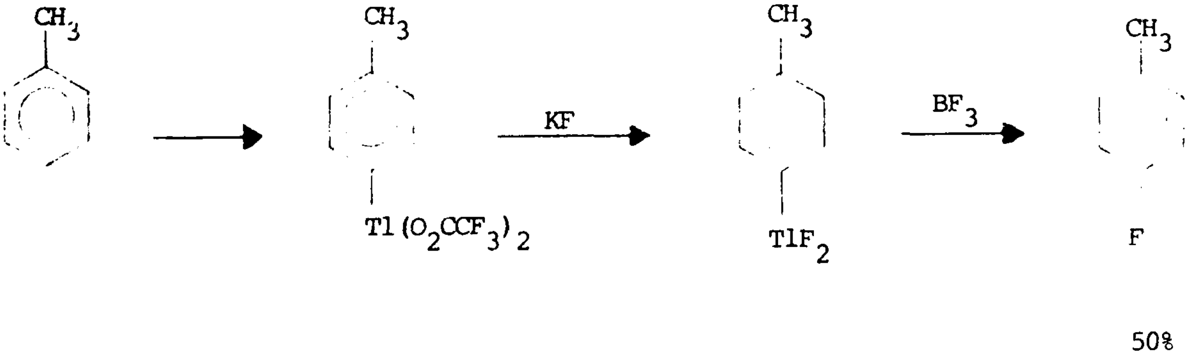

(4)

In 1962, Neil Bartlett discovered that xenon was not inert. Shortly thereafter, several fluorides of xenon were prepared and their chemical properties were studied. It was determined that xenon difluoride in the presence of anhydrous HF catalyst was an effective fluorinating agent[14,15] for aromatic compounds (Equation 5). Although this reaction is not regiospecific, it is tolerant to a wide variety of functional groups. Xenon difluoride in the presence of HF has also been shown to fluorinate alkenes. Shackelford and coworkers[16] have shown that anhydrous HF can be replaced by boron trifluoride etherate complex for the fluorination of alkenes (Equation 6). Shackelford's modification also allows for the use of conventional laboratory equipment in the fluorination reactions.

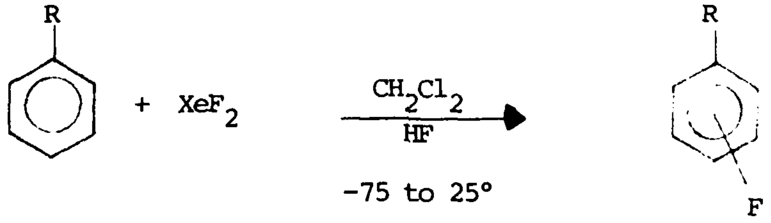

(5)

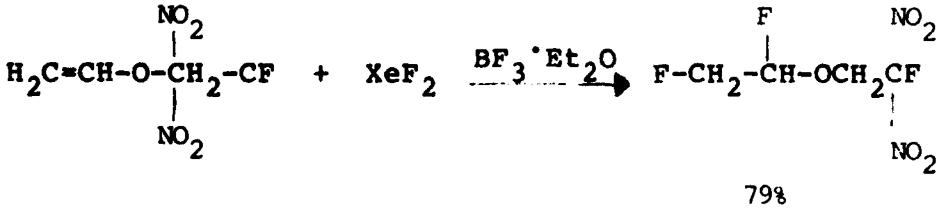

$$H_2C{=}CH{-}O{-}\overset{NO_2}{\underset{NO_2}{CH_2}}{-}CF \; + \; XeF_2 \; \xrightarrow{BF_3{\cdot}Et_2O} \; F{-}CH_2{-}\overset{F}{CH}{-}OCH_2\overset{NO_2}{\underset{NO_2}{CF}} \qquad (6)$$

79%

M. Schlosser[17] has demonstrated that aryllithium compounds react with perchlorofluoride to give the arylfluorides in moderate yields (Equation 7).

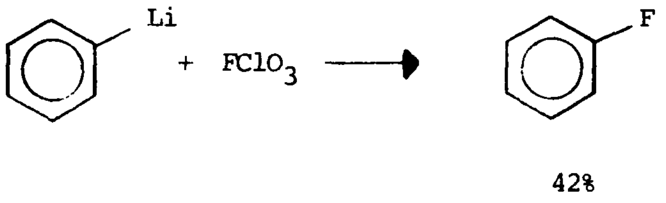

(7)

Recently it has also been demonstrated that under the appropriate conditions xenon difluoride can act as a source of positive fluorine.[18]

It is well known in the literature that an aromatic nucleus can be regiospecifically metallated either by direct metalation with an alkyllithium or by lithium-halogen exchange on the appropriately substituted arene.[21,22,23,24,25] Likewise, the aryl Grignards, cuprates, and cadmium compounds are similarly available, utilizing standard laboratory procedures. Using these organometallics and xenon difluoride as a positive fluorine source, it is reasonable to expect the desired regiospecific fluoroaromatics.

RESULTS AND DISCUSSION

Organolithiums were chosen for the initial phase of our investigation. Aromatic compounds may be metallated easily by one of two methods (Equations 8, 9).[23,25]

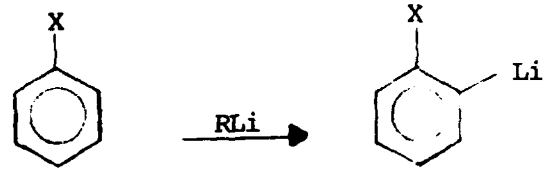

R = alkyl, aryl, NR_2 (8)

X = 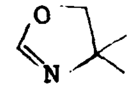 (Ref. 21, 28, 29)

X = 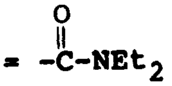 $-\overset{O}{\overset{\|}{C}}-NEt_2$ (Ref. 30)

X = $-CH(OEt)_2$ (Ref. 31)

X = 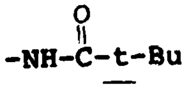 $-NH-\overset{O}{\overset{\|}{C}}-\underline{t}-Bu$ (Ref. 32)

X = amine (Ref. 33)

X = $-O-CH_2-O-CH_{23}$ (Ref. 34)

X = 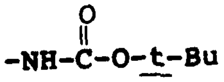 $-NH-\overset{O}{\overset{\|}{C}}-O-\underline{t}-Bu$ (Ref. 35)

R = alkyl, aryl (9)

X = NMe_2, NO_2, CO_2H, NH_2 (Ref. 24)

X = -CN (Ref. 24)

X = $-CO_2H$ (Ref. 36)

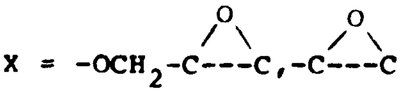

$$X = -OCH_2-\overset{O}{C\text{---}C}, -\overset{O}{C\text{---}C} \quad \text{(Ref. 37)}$$

X = $-CO_2R$ (Ref. 38)

X = $-(CH_2)_nCl$, $(CH_2)_nBr$ (n = 1,2,3) (Ref. 39)

These methods offer not only regiospecificity but also ease of preparation and compatibility with a wide spectrum of functional groups, especially the nitro groups (Equation 9).

The model system chosen for our preliminary investigations is phenyllithium. The initial results of this study are shown in Table I. Analysis of the reaction mixtures was accomplished by using GC/mass spectral techniques. The highest yield to date (entry 10, Table I) is 16% (nitrobenzene relative to benzene). This reaction has not been optimized and work is in progress to increase its synthetic utility. The interaction of solvent, temperature, and catalysts are also being investigated. Its extension to other model systems (Equation 8, 9) and other organometallics is currently under investigation.

TABLE I

REACTION OF PHENYLLITHIUM WITH XENON DIFLUORIDE

Entry	Solvent	Temperature °C	Complexing Agent	Comments
1	Et_2O	-78, 2Hr; RT overnight	--	No PhF
2	Et_2O	0, 30 min[h]	--	No PhF
3	Et_2O	0, 3Hr, RT	$BF_3 \cdot Et_2O$	No PhF, addition of $BF_3 \cdot Et_2O$ gave black residue residue after 10 min at 0°
4	Et_2O	-78, 2Hr; -45, 4.5 Hr; -25, 1Hr; -25 to Rt, overnight	$BF_3 \cdot Et_2O$	Trace PhF
5	cyclohexane	RT, 1 Hr	--	PhLi not added, XeF_2 reacted with solvent[b]
6	cyclohexane	0 to 10; RT	--	No PhF, XeF_2 "appeared" to react with solvent[b]
7	n-hexane	-78, 1 Hr;[c] -78, 2,25Hr; -78 to RT overnight	$BF_3 \cdot Et_2O$	12.3% PhF[d]
8	n-hexane	-78, 1Hr;[e]	$BF_3 \cdot Et_2O$	Trace PhF
9	THF	-78 to RT	$BF_3 \cdot Et_2O$	No PhF, XeF_2 reacted with solvent
10	pentane	-100, 1Hr;[f] -100, 1.25 Hr; -78 to RT overnight	$BF_3 \cdot Et_2O$	16% PhF[d]
11	THF	-78, 3Hr; -78 to RT overnight	$BF_3 \cdot Et_2O$	No PhF[g]

12	Et_2O	0, 3Hr	i	No PhF

(a) Phenyllithium injected at -25 and reaction allowed to warm to room temperature; (b) Analysis of the reaction of XeF_2 with cyclohexane in a separate experiment show the presence of fluorocyclohexane; (c) PhLi added after 1 Hr at -78; (d) Ratio PhF relative to PhH; (e) Reaction warmed to -25 to partially dissolve XeF_2-boron complex then cooled to -55; PhLi added and Rxn stirred at room temperature overnight; (f) PhLi added after 1 Hr at -100; (g) Several unidentified high molecular weight materials present in reaction mixture; (h) Reaction at 0°C for 6 Hr gave no PhF; (i) PhLi complexed with TMEDA before addition to XeF_2.

Time, temperature, solvent, and catalyst studies have provided several initial results which are noteworthy. Halocarbon solvents have usually been the solvent of choice for xenon difluoride/aromatic reactions.[14,15] At room temperature it is known that methylene choloride reacts with xenon difluoride.[18] We have additionally found that at 0°C to room temperature that xenon difluoride reacts with hydrocarbons to give fluorinated materials (cyclohexane converted to fluorocyclohexane). In ether and THF solvents xenon difluoride is soluble in varying degrees over the temperature range of -78°C to room temperature. The addition of boron trifluoride etherate seems to increase the solubility of the xenon difluoride in solvents, presumably by formation of the xenon difluoride-boron complex. However, warming of these mixtures in the presence of organolithiums gives black materials. Analysis of the product mixtures also show several products arising from reaction of the phenyllithium with solvent. This is not surprising and while it is an undesirable side reaction, it is not without precedence in the literature.[19,20]

Several reactions have been run using grignard reagents but initial results have not been examined in enough detail to make comments at this time.

CONCLUSION

There are few methods available for preparing monofluorinated aromatics. Of these methods, most of them give mixtures of products; require special equipment for the handling of toxic, corrosive, or explosive materials; and only give moderate yields. The work in progress promises to provide for a synthesis of fluoroaromatics which should eliminate the above limitations. In addition, the application of this methodology will provide for routes into previously difficult to obtain compounds and also furnish the foundation for its extension into the area of aliphatic chemistry.

EXPERIMENTAL PROCEDURES

General

All temperatures are in degrees Celsius (^{o}C). Gas chromatographic data were taken on a Varian model 2700 series GC with a thermal conductivity detector using a 6′ x 1/8" stainless steel column packed with 10% FFAP on 60/80 mesh Chromosorb W. The column temperature was 73^{o} and the carrier gas was helium at 20 Psig and 14 on the flowmeter. Mass spectral analysis was run on a Hewlett Packard Model 5985 GC/Mass Spec using a 3′ x (6 mm OD, 2 mm ID) glass column packed with 2% OV-101 on 100/120 mesh Ultrabond 20M. The xenon difluoride was transferred to the reaction flask in a drybox. All reactions were run on the bench top under an argon atmosphere. All glassware was baked at 125^{o} for a minimum of 1 hour, then allowed to cool in a desiccator.

Solvents and Reagents

Tetrahydrofuran and ether were distilled from the sodium benzophenone ketone immediately before use. The hydrocarbon solvents were dried by distillation from calcium hydride. The TMEDA was distilled from calcium hydride and stored under an inert atmosphere. The boron trifluoride etherate was purified according to Fieser.[26] The organolithiums were standardized using 2,5-dimethoxybenzyl alcohol.[27]

Typical Procedure for the Reaction of Xenon Difluoride with Organolithiums

Xenon difluoride (0.212 g, 1.25 mmol) was placed in a 25 mL flask with a stir pea in the drybox. The flask was capped with a rubber septum and transferred out of the drybox to the bench top (argon atmosphere). The reaction flask was cooled to -100° (ether/liquid nitrogen bath) and 5.0 mL of pentane was added. Boron trifluoride etherate (0.15 mL, 1.22 mmol) was added and the reaction mixture was stirred at -100° for 1 hour. Phenyllithium (1.92 M in cyclohexane, 0.69 mL, 1.32 mmol) was added and the mixture was stirred at -100° for 1.25 hours (light creamy tan color). The reaction temperature bath was raised to -78° (solid CO_2 added) and the reaction allowed to warm to room temperature overnight. Aqueous sodium fluoride solution (2.5 g/100 mL, 6 mL) was added and the mixture extracted with ether. The organic phase was dried over anhydrous magnesium sulfate and filtered. The dried organic phase was subjected to GC/mass spectral analysis and showed 16% fluorobenzene (relative to benzene).

Acknowledgement. The authors wish to thank Mr. Lloyd Pflug, FJSRL, for the GC/mass spec analyses, without which this work would not have been possible.

REFERENCES

1. A.I. Meyers and B.F. Williams, Tet. Lett., 223 (1978).

2. P.A.J. Jansen, C. van de Westfringh, A.H.M. Jageneau, P.J.A. Demoen, B.K.F. Hermans, G.H.P. van Daele, K.H.L. Schellerens, C.A.M. van der Eycken, and C.J.E. Niemegeers, J. Med. Pharm. Chem., 1, 281 (1959).

3. D. Lednicer and L.A. Mitscher, Organic Chemistry of Drug Synthesis, 1977, John Wiley and Sons, New York.

4. J. Hannah, W.V. Ruyle, H. Jones, A.R. Matzuk, K.W. Kelly, B.E. Witzel, W.J. Holtz, R.A. Houser, T.Y.Shen, L.H. Sarett, V.J. Lotti, E.A. Risley, C.G. van Arman, and C.A. Winter, J. Med. Chem., 21, 1093 (1978).

5. M.S. Newman, J.H. Cecil and W.M. Hung, J. Med. Chem., 15, 569 (1972).

6. J.M. Tedder, Adv. in Fluorine Chem., 2, 104 (1961).

7. S. Nagasi, Fluorine Chem. Rev., 1, 77 (1967).

8. J. Burdon, I.W. Parsons, and J.C. Tatlow, Tetrahedron, 28, 43 (1972).

9. A. Roe, Organic Reactions, 5, 193 (1949).

10. H. Suschitzky, Adv. in Fluorine Chem., 4, 1 (1965).

11. H.B. Gottlieb, J. Am. Chem. Soc., 58, 532 (1936).

12. D.M. Mulvey, A.M. DeMarco, and L.M. Weinstock, Tet. Lett., 1419 (1978).

13. E.C. Taylor, E.C. Bigham, and D.K. Johnson, J. Org. Chem., 42, 362 (1977).

14. M.J. Shaw, H.H. Hyman, and R. Filler, J. Am. Chem. Soc., 91, 1563 (1969).

15. Ibid., 92, 6498 (1970).

16. S.A. Shackelford, R.R. McGuire, and J.L. Pflug, Tet. Lett., 363 (1977).

17. M. Schlosser and G. Heinz, Chem. Ber., 102, 1944 (1969).

18. T. Tsushima, K. Kawada, and T. Tsuji, Tet. Lett., 23, 1165 (1982); S.A. Shackelford, J. Org. Chem., 44, 3485 (1979).

19. T.N. Bocharova, N.G. Marchenkova, L.D. Shustov, T.Y. Prokof´eva, and L.N. Nikolenko, Zh. Obshch, Kim., 43, 1325 (1973); L.D. Shustov, T.N. Bocharova, T.I. Yurasova, N.G. Marchenkova, V.A. Legasov, and L.N. Nikolenko, Zn. Obshch. Kim., 43, 841 (1973).

20. M. Zupan and A. Pollak, J. Fluorine Chem., 7, 443 (1976).

21. A.I. Meyers and E.D. Mihelich, J. Org. Chem., 40, 3158 (1975); H.W. Gschwend and A. Hamdan, J. Org. Chem., 40, 2008 (1975).

22. P. Beak and R.A. Brown, J. Org. Chem., 42, 1823 (1977).

23. H.W. Gschwend and H.R. Rodriguez, Organic Reactions, 26, 1, (1979).

24. W.E. Parham and R.M. Piccirilli, J. Org. Chem., 42, 257 (1977); W.E. Parham and C.D. Jones, J. Org. Chem., 41, 1187 (1976).

25. (a) P. Beak and D.B. Reitz, Chem Rev., 78, 275 (1978); (b) H. Gilman and J.W. Morton, Jr., Org. Reactions, 8, 258 (1954); (c) B.J. Wakefield, The Chemistry of Organolithium Compounds, Pergamon Press, New York, 1974, Chapter 3,4; (d) D.W. Slocum and C.A. Jennings, J. Org. Chem., 41, 3653 (1976).

26. L.F. Fieser and M. Fieser, Reagents for Organic Synthesis, Volume 1, page 70, John Wiley and Sons Inc., New York, 1967.

27. M.R. Winkle, J.M. Lansinger, and R.C. Ronald, J. Chem. Soc., Chem Comm., 87 (1980).

28. A.I. Meyers and K. Lutomski, J. Org. Chem., 44, 4465 (1979).

29. A.I. Meyers and W.B. Avila, Tet. Lett., 21, 3335 (1980).

30. P. Beak and R.A. Brown, J. Org. Chem., 44, 4463 (1979); Ibid, J. Org. Chem., 42, 1823 (1977).

31. H.P. Plauman, B.A. Keay, and R. Rodrigo, Tet. Lett., 4921 (1979).

32. W. Fuhrer and H.W. Gschwend, J. Org. Chem., 44, 1133 (1979).

33. G. Friedmann, P. Linder, M. Brini, and A. Cheminat, J. Org. Chem., 44, 237 (1979).

34. R.C. Ronald, Washington State University, Pullman, Washington,

private communication.

35. J.M. Muchowshi and M.C. Venuti, Abstract 108, Second Chemical Congress of the North American Continent, San Francisco, California, August 25-29, 1980.

36. W.E. Parham and Y.A. Sayed, *J. Org. Chem.*, *39*, 2051 (1974).

37. K.L. Dhawan, B.D. Gowland, and T. Durst, *J. Org. Chem.*, *45*, 922 (1980); C.K. Bradsher and D.C. Reams, *J. Org. Chem.*, *43*, 3800 (1978).

38. W.E. Parham and L.D. Jones, *J. Org. Chem.*, *41*, 2705 (1976).

39. P.D. Brewer, J. Tagat, C.A. Hergrueter, and P. Helquist, *Tet. Lett.*, 4573 (1977); W.E. Parham, L.D. Jones, and Y.A. Sayed, *J. Org. Chem.*, *41*, 1184 (1976).

Chapter 2

CORRELATION OF MOLECULAR ORBITAL CALCULATIONS WITH MASS SPECTRA FOR 1-NITROPROPENE

by Kenneth M. Dieter and Larry P. Davis

INTRODUCTION

The thermal decomposition mechanism of 2,4,6-trinitrotoluene (TNT) (1) has never been firmly established. The first step in this process is thought to possibly involve the intramolecular transfer of a hydrogen atom from a methyl carbon to an oxygen of the nitro group.

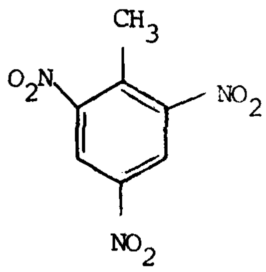

1

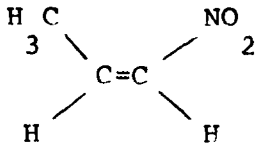

2

Cis-1-nitropropene (C-1-NP) (2) was selected as a model compound for experimental and theoretical studies of this problem based on its similarity to the active portion of the TNT molecule.

The electron impact mass spectra of cis- and trans-1-nitropropene offer potentially significant data for these studies. The fragmentation occurring in the mass spectrometer is a function of the chemical reactivity of various sites in the molecule. Consequently, the fragmentation pattern and relative abundances of the various fragment ions yield information on the relative reactivities of these sites.

To substantiate the conclusions drawn from these spectra, molecular orbital calculations were performed on selective fragmentation pathways, and their results correlated with spectral data.

EXPERIMENTAL

The mass spectra of C-1-NP and trans-1-nitropropene (T-1-NP) (3) in diethyl ether were

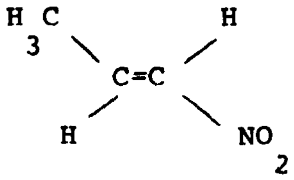

3

run in a Hewlett-Packard Model 5985 gas chromatograph/mass spectrometer operating at an ionizing energy of 70 eV. Although the barrier to rotation around the double bond is predicted by calculations to be relatively small (approximately 20 kcal/mol in the neutral molecule), the two spectra are significantly different.

(Figures 1 and 2). The parent peak (M/Z 87) is the base peak for T-1-NP while M/Z 39 is the base peak for C-1-NP and M/Z 87 has a relative abundance of only 21.4. Most significant in its ultimate application to the TNT studies is the presence of a sizeable peak at M/Z 70 in the C-1-NP spectrum (rel. ab. 21.2) and the absence of a similar peak in the T-1-NP. This peak indicates the loss of an OH radical, the logical conclusion being that an intramolecular hydrogen transfer does occur in C-1-NP but not in T-1-NP. An extension of this conclusion, then, would be that the hydrogen must come from the methyl group, similar to what is suspected to occur in TNT. These conclusions were tested in the theoretical investigation.

THEORETICAL PROCEDURE

The calculations were carried out using the restricted Hartree-Fock version of the MNDO procedure. Equilibrium geometries were found by minimizing energy with respect to all geometric variables. All transition state energies are approximate values based on results from reaction path calculations and incomplete refinement in a transition state optimization routine which minimizes the gradient norm.

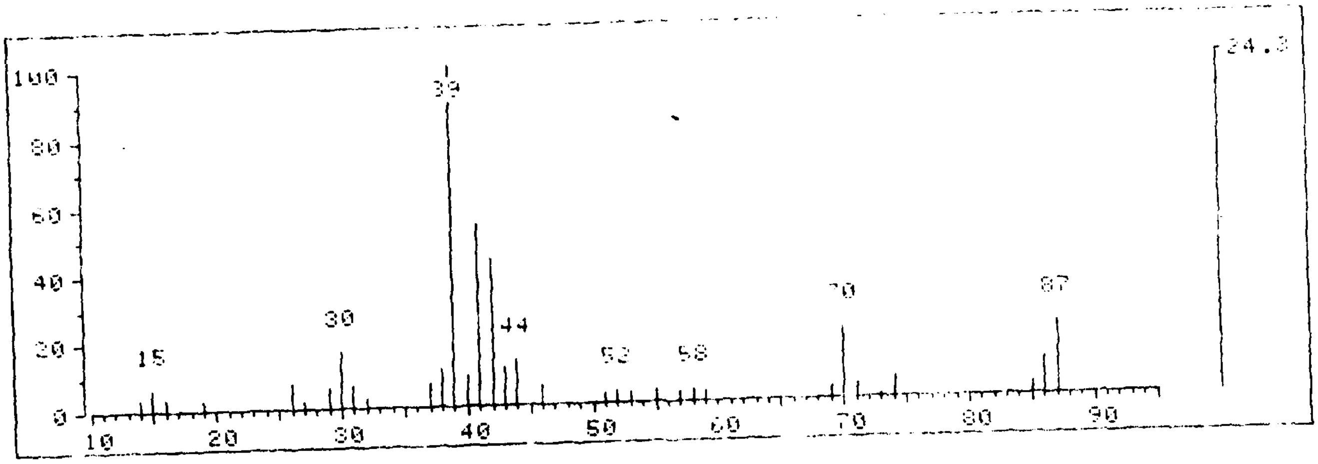

M/Z	REL ABUND	M/Z	REL ABUND	M/Z	REL ABUND	M/Z	REL ABUND
14	3.8	32	2.9	46	5.5	70	21.2
15	6.7	37	7.2	51	3.2	71	4.3
16	3.5	38	11.6	52	4.1	73	.6
19	3.2	39	100.0	53	3.2	74	6.4
26	7.8	40	9.0	55	3.8	85	3.5
27	2.3	41	53.9	57	3.2	86	11.3
29	6.4	42	43.5	58	3.8	87	21.4
30	17.1	43	11.0	59	2.9		
31	6.4	44	13.6	69	3.5		

Figure 1. Mass Spectrum of Cis-1-Nitropropene

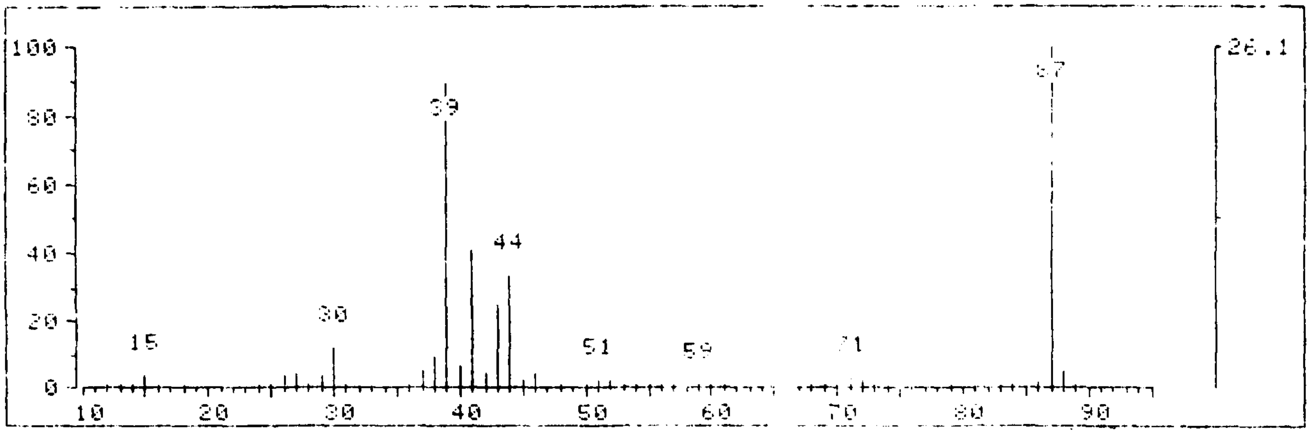

M/Z	REL ABUND	M/Z	REL ABUND	M/Z	REL ABUND	M/Z	REL ABUND
12	.4	36	.7	52	2.1	72	2.4
13	.3	37	5.1	53	1.1	73	.4
14	.3	38	9.4	54	.7	74	1.2
15	3.6	39	89.7	55	1.1	75	.1
16	.8	40	6.2	56	.6	79	.2
18	.3	41	40.9	57	.4	83	.2
24	.3	42	4.3	58	.4	84	.2
25	.9	43	24.7	59	1.3	86	1.9
26	3.9	44	33.1	60	.0	87	100.0
27	4.1	45	2.7	61	.2	88	4.8
28	1.0	46	4.6	68	.5	89	.6
29	3.9	48	.3	69	1.0		
30	12.2	50	.6	70	.7		
31	.2	51	2.4	71	3.0		

Figure 2. Mass Spectrum of Trans-1-Nitropropene

The potential fragmentation pathways of C-1-NP investigated were the transfer of hydrogen atoms from the three carbons to an oxygen of the nitrogen group, the dissociation of a hydroxyl radical or cation from the products of the hydrogen transfers, the dissociation of hydrogen atoms or cations from the three carbons, the dissociation of an oxygen atom or cation, the dissociation of a CH_3 radical or cation, and the dissociation of an NO_2 radical or cation. These fragmentations were chosen because they were straightforward and, except for the hydrogen transfer, required no rearrangement. Additionally, with the exception of the NO_2 dissociation, all fragmentation resulted in high M/Z fragments, thereby avoiding ambiguities inherent in trying to interpret fragmentation paths to lower M/Z values due to the high probability of rearrangements.

The only fragmentation of T-1-NP investigated was the transfer of a hydrogen from carbon-2 to an oxygen of the nitro group and the subsequent dissociation of a hydroxyl radical or cation. This fragmentation was chosen due the significance of the M/Z 70 peak appearing in the C-1-NP spectrum and not in the T-1-NP spectrum.

The cations of C-1-NP and T-1-NP were optimized first. All geometries input for the optimization of the fragments were ultimately based on the optimized geometries of C-1-NP and T-1-NP cations.

RESULTS AND DISCUSSION

The results of the calculations are presented in Table 1.

Table 1. Energies of 1-Nitropropene Fragmentation Pathways

A. Cis-1-Nitropropene

	Heats of Formation (kcal/mol)				
	Reactant	Product(s)	Reaction	Transition State	Energy of Activation (kcal/mol)
H Transfer to Nitro Group					
From C_1	263.6	245.0	-18.6	~333*	~69
From C_2	263.6	240.9	-22.8	~317	~53
From C_3	263.6	221.5	-42.1	~282	~18
OH Radical Dissociation after H Transfer to Nitro Group					
H From C_1	245.0	260.6	15.6		
H From C_2	240.9	261.0	20.1		
H From C_3	221.5	243.3	21.8	>290**	>68
OH^+ Dissociation after H Transfer to Nitro Group					
H From C_1	245.0	363.5	123.5		
H From C_2	240.9	366.9	126.0		
H From C_3	221.5	353.5	132.0		

H Atom Dissociation					
From C_1	263.6	351.2	87.6	>360	>96
From C_2	263.6	332.2	68.6	>345	>81
From C_3	263.6	312.2	48.6	>326	>62
H^+ Dissociation					
From C_1	263.6	439.1	175.5		
From C_2	263.6	431.5	167.9		
From C_3	263.6	417.6	154.0		
O Atom Dissociation	263.6	289.3	25.7	>304	>40
O^+ Dissociation	263.6	384.4	120.8		
CH_3 Radical Dissociation	263.6	332.9	69.3		
CH_3^+ Dissociation	263.6	322.2	58.6	~324	~60
NO_2 Radical Dissociation	263.6	247.7	-15.9	>280	>16
NO_2^+ Dissociation	263.6	294.1	30.5		
B. Trans-1-Nitropropene					
H Transfer to Nitro Group					
From C_2	263.3	240.6	-22.7	>306	>42

OH Radical Dissociation after H Transfer to Nitro Group					
From C_2	240.6	261.1	20.5	>299	>58
OH^+ Dissociation after H Transfer to Nitro Group					
From C_2	240.6	366.9	126.3		

* ~ indicates best estimate to-date, from transition state optimization routines in which gradients were not fully minimized.

** > indicates best estimate to-date, from a reaction path calculation. This calculation has not yet been entered into the transition state optimization routine.

NOTE: Heat of Formation values for OH, OH^+, H, H^+ and O were obtained from the JANAF Thermochemical Tables, Dow Chemical Company, Midland, MI. The Heat of Formation value for O^+ was based on the JANAF table value for O and the ionization potential of oxygen from Inorganic Chemistry, James J. Huheey, 2nd Ed., pg 40.

As expected, the hydrogen transfer from the methyl carbon to the nitro group is highly favored, both kinetically and thermodynamically, over the transfer from the other carbons. Once the hydrogen is bonded to an oxygen of the nitro group, OH dissociation is slightly favored if the hydrogen had originally been bonded to carbon-1 rather than carbon-3. However, the hydrogen transfer reaction is the overriding factor, heavily favoring the hydrogen coming from carbon-3.

Results of the hydrogen transfer from carbon-2 of T-1-NP and the subsequent loss of an OH radical substantiate this conclusion. Again, transfer of a hydrogen from carbon-3 is kinetically and thermodynamically favored over transfer from carbon-2 of T-1-NP. Similarly, once the hydrogen transfer is accomplished, OH loss is slightly favored if the hydrogen originated on carbon-2 of T-1-NP.

The fact that the C-1-NP spectrum has an M/Z 70 peak and the T-1-NP spectrum doesn't indicates the hydrogen transfer is the critical step.

Of all the fragmentations investigated, the most favored one is the loss of an NO_2 radical. This fragmentation is predicted to be exothermic and to have an activation energy significantly lower than the hydrogen transfer from carbon-3 and subsequent loss of an OH radical. The higher relative abundance of M/Z 41 compared with M/Z 70 (53.9 vs 21.2) would be expected based on these results.

Even the relative abundance of these two peaks may not indicate the full extent to which the NO_2 loss is favored over other fragmentations. The base peak, M/Z 39, is from a $C_3H_3^+$ fragment. The most stable $C_3H_3^+$ fragment is the allyl cation (ΔH_f = 265.0 kcal/mol). A logical path to this fragment would involve the loss of the NO_2 radical followed by the loss of an H_2 molecule comprised of one hydrogen atom from carbon-2 and the other from carbon-3. The overall heat of these reactions would then be 1.4 kcal/mol and the activation energies in all likelihood would be small.

Results of calculations on other fragmentations also agree well with the observed mass spectrum of C-1-NP. Of the possible hydrogen dissociations, loss from carbon-3 is favored. It has a higher heat of reaction than the favored hydrogen transfer/OH loss, and as might be expected, the M/Z 86 peak is smaller than the M/Z 70 peak (11.3

vs 21.2). Although the activation energy for the hydrogen dissociation is lower than that of the OH dissociation, the hydrogen dissociation does not have the benefit of an exothermic first step. Similarly, CH_3 dissociation favors the methyl group carrying the positive charge, and there is an M/Z 15 peak and not an M/Z 72 peak in the C-1-NP spectrum. While the activation energies for the loss of CH_3^+ and hydrogen dissociation from carbon-3 are very close, the heat of reaction for the CH_3 dissociation is 10 kcal/mol higher than that for the hydrogen dissociation.

The only apparent anomaly appears to be the dissociation of an oxygen atom. Despite a relatively low heat of reaction and a lower activation energy than the most favored hydrogen dissociation, methyl and hydrogen transfer and hydroxyl dissociation, the relative abundance of M/Z 71 is only 4.3. However, the enthalpy gradient for the loss of an oxygen atom is extremely large around the transition state (over 100 kcal/A). The actual heat of formation of the transition state and, consequently, the activation energy may be significantly larger than indicated.

CONCLUSION

The results of theoretical calculations do appear to justify the apparent fragmentation pattern in the C-1-NP mass spectrum. However, further work needs to be accomplished to finalize this study. All transition states must be optimized and thermodynamic calculations performed on them. The quasiequilibrium theory, widely accepted as explaining mass spectral fragmentation, can then be employed to check our conclusions.

The question of thermodynamic versus kinetic control must also be answered. Comparison of NO_2 radical loss versus hydrogen transfer from carbon-3 seems to point toward kinetic control. Comparison of methyl cation loss with hydrogen dissociation from carbon-3, however, seems to lean toward thermodynamic control. Again, full optimization of transition states and application of the quasiequilibrium theory may provide the answer.

Finally, the loss of H_2 after NO_2 dissociation should be investigated. Additionally rearrangement of the nitro group to a nitroso group followed by loss of NO would be an interesting study for comparing C-1-NP and T-1-NP spectra.

Acknowledgements. The authors wish to thank Mr. Lloyd Pflug, FJSRL, for the GC/mass spec analyses. Also, Dr. Almon G. Turner, University of Detroit, was kind enough to provide us with the sample of 1-nitropropene which he had synthesized.

Chapter 3

Synthesis of Polymers for Laser Damage Testing

by Alan A. Shaffer

ABSTRACT

Methyl methacrylate polymers have been prepared (by bulk free-radical initiation) to determine their laser damage resistance properties. Important variables examined include plasticizer loadings, purity, and sample preparation methods. The key relationship sought is whether an increased viscoelasticity of the polymer structure allows it to dissipate laser energy more efficiently, thus improving its damage resistance. Also, purification of all monomers is important to exclude foreign occlusions that would otherwise be prime energy-absorbing centers. Sample recipes and purification methods are discussed.

INTRODUCTION

Research pioneered by A.A. Manenkov (P.N. Lebedev Physics Institute, Academy of Sciences of the USSR) has demonstrated good laser damage resistance of poly methylmethacrylate (PMMA) materials. The goal of our research is to optimize PMMA laser damage resistance by variation of structure and molecular weight and to investigate the laser damage resistance of various other common plastics, including polycarbonate.

The prospect of laser compatibility with plastics greatly increases the flexibility of designing new laser detection and weapon systems. Several inherent advantages would include the greater ease and lower cost of fabricating components out of plastics rather than glass or metal. Also, Q-switches and dyes could be more easily incorporated into the polymer matrix to alter or control laser wavelength and power. In addition, passive defense against laser damage would be enhanced.

The literature (primarily involving Manenkov's research) discusses the relative laser damage resistance of several PMMA samples, many including copolymers derived from methyl methacrylate (MMA) and other acrylate monomers. Once laser damage testing begins, a specific correlation will be sought between structure and laser damage resistance. Important variables here include molecular weight, plasticizer loadings, purity, and sample preparation. An important feature contributing to laser damage resistance is thought to be the polymer's ability to dissipate efficiently laser energy from a focal point. The key mechanism for this is believed to be thermal micro-Brownian motion of macro-molecular segments. From this perspective, PMMA samples varying in copolymer composition will be investigated. The monomer additive generally will provide a linear pendant moeity to serve as a kind of intramolecular plasticizer. Also, non-reactive plasticizers like dibutyl phthalate will be used for direct comparison. This may give us greater insight to the role of plasticization in enhancing laser damage resistance.

DISCUSSION

Initial attempts to prepare poly methylmethacrylate (PMMA) by anionic solution polymerization failed to provide samples that could be fabricated for laser testing. Annealing under vacuum was unsuccessful. This polymerization method was thus abandoned.

Bulk polymerization (no solvent) by free-radical initiation of methyl methacrylate monomer (MMA) within expendable glass ampule reaction vessels has given solid cylindrical samples having good optical clarity. Generation of voids within the sample (due to nitrogen evolution from decomposition of the azoisobutyronitrile (AIBN) catalyst) has been a recurrent problem particularly in the larger size runs (using 10-12g MMA). Generally, this can be avoided by using low levels (~ one weight percent with respect to MMA) of plasticizer which presumably lowers the viscosity of the liquid during polymerization allowing the bubbles to reach the surface. With this modification, solid void-free cylindrical samples with 0.63-inch diameters and up to two-inch lengths have been obtained. Due to surface imperfections of the glass ampule, these samples will need to be cut and polished prior to laser testing. These samples are thick enough to allow meaningful statistical data to be obtained for laser <u>bulk</u> damage threshold determination. Conditions are presently being sought to provide a void-free sample of neat poly methylmethacrylate (PMMA). This material is needed as a reference for evaluating modified PMMA samples.

A series of PMMA samples have also been prepared using 5 to 20 weight percent (with respect to MMA) of reactive and inert plasticizers. These materials would presumably increase the flexibility of the polymer system by enhancing inter chain mobility (inert plasticizers) or intra/inter chain mobility (reactive plasticizers). This greater viscoelasticity should provide a better way to dissipate laser energy presumably increasing damage resistance. But there probably is a point of diminishing returns; to determine that point is one of our research goals.

A typical sample recipe follows:

- 10-12g MMA
- azoisobutyronitrile (AIBN) catalyst
  (0.01-0.2 weight percent with respect to MMA)
- plasticizer (1-20 weight percent with respect to MMA)
  - reactive acrylate comonomer (one of the following):
    - n-butyl acrylate
    - ethyl acrylate
    - isodecyl methacrylate

  or

  - non-reactive material (one of the following):
    - dibutyl phthalate
    - ethanol
    - poly lauryl methacrylate
- heating at 40 -> 80^{o}C for 3-6 days in sealed ampule
  (gradual T increase)

Another important criterion for a meaningful evaluation of laser damage resistance is polymer clarity and homogeneity. Dust-free samples are needed to assess the effect of laser energy on the polymer without interference from energy absorption by foreign occlusions. Samples have been prepared using both purified MMA (treated with calcium hydride followed by vacuum distillation or distillation under nitrogen atmosphere) and MMA directly from the can. Most of the samples prepared using the purified MMA showed under 20X magnification a modelled interference pattern when a helium laser beam was passed through the samples. This indicated fairly clean, homogeneous material. Samples prepared from unpurified MMA will be examined the same way to see if any real difference exists between the samples. Milli-pore filters are presently on order for purification of all liquid reagents. Depending on how the polymer samples look after milli-pore filtration of the monomers, this may be the only purification step required.

Up to now, laser damage testing has focused on commercially available optical-grade plastics, including PMMA and polycarbonate. Soon, damage testing will begin on the experimental PMMA samples prepared in this work. Future direction of the synthesis effort will depend on these results, possibly including the preparation of polycarbonate.

Chapter 4

USE OF MOLECULAR ORBITAL CALCULATIONS TO MODEL TNT THERMOCHEMICAL DECOMPOSITION

by Larry P. Davis and Almon G. Turner

ABSTRACT

We have used 1-nitropropene as a model compound to study TNT decomposition. Utilizing Dewar's MNDO and MINDO/3 methods, several potential first steps in the thermochemical decomposition of TNT have been tested theoretically against known experimental kinetic parameters. Calculated ΔH^{o}'s for the processes indicate that 1-nitropropene is a valid model for use in studying TNT decomposition. Results show that several processes appear to be quite feasible as a possible initial step in the decomposition. Principal among these is the intermolecular hydrogen transfer from the methyl group of one molecule to a nitro group of a second molecule.

INTRODUCTION

Semi-empirical molecular orbital calculations based upon the MNDO[1] and MINDO/3 approximations[2] have been successfully used to estimate the enthalpy of activation and to provide information about the nature of the transition state involved in a chemical reaction for a wide variety of chemical systems.[3] This laboratory has been concerned with kinetic studies of the thermal decomposition of 2,4,6-trinitrotoluene (TNT) for the past several years.

Isothermal differential scanning calorimeter studies (IDSC) showed a substantial (~1.7) kinetic isotope effect present upon methyl group deuteration.[4] Electron paramagnetic resonance (EPR) studies showed conclusively that radicals are present in the initial and later stages of the thermochemical decomposition of TNT, and measurements of the intensity of the radical signals as functions of time and temperature produced an activation energy of 40.9 kcal mol^{-1} for the early radical-producing step in the decomposition.[5] Monitoring the signal of a later radical produced during the bulk phase decomposition gave a bulk phase decomposition activation energy of 30.2 kcal mol^{-1}. The initial radical produced has an EPR spectrum consistent with a molecule having 5 equivalent hydrogen atoms and 2 equivalent nitrogen atoms.[6]

We recently decided to initiate the theoretical study of several alternative decomposition reaction channels for the TNT system. The large number of internal coordinates necessary to specify the geometry of the TNT molecule ($3N-6 = 60$) and the trial and error nature of the process involved in identification of the reaction coordinate for a given reaction step[7] dictated that the calculations could be expected to be lengthy, time-consuming, and relatively expensive. Accordingly, we decided to seek out a smaller, simpler system which might hopefully reflect the same behavior as TNT. We selected the 1-nitropropene molecule. This molecule, possessing the salient structural elements of the TNT molecule, might be expected to provide an accurate reflection of the TNT system provided the decomposition reactions considered are not dominated by electronic factors directly traceable to the conjugation effects present in the

TNT ring.

REACTION MECHANISMS

On the basis of the experimental data available to us the following six decomposition channels were considered.

1. Intramolecular Hydrogen Transfer

   1-nitropropene ->

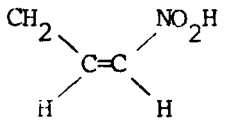

2. Intermolecular Hydrogen Transfer

   2 (1-nitropropene) ->

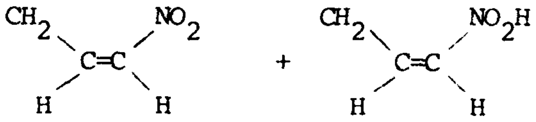

3. Intramolecular Oxygen Insertion

   1-nitropropene ->

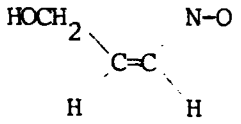

4. Intermolecular Oxygen Insertion

   2 (1-nitropropene) ->

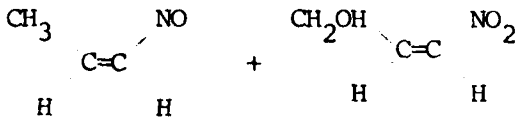

5. Nitro-Nitrite Rearrangement

   1-nitropropene ->

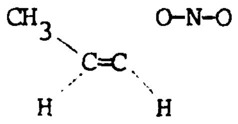

6. Nitro Group Removal

   1-nitropropene ->

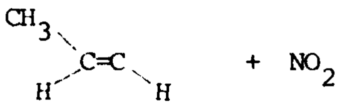

CALCULATIONS

MNDO and MINDO/3 calculations were carried out for 1-nitropropene and each of the product molecules occurring in the preceding six mechanisms, as well as their TNT analogs. The energy of each molecule was calculated as a function of its geometry and the geometry of lowest energy determined, i.e., a full geometry optimization was carried out. The unrestricted Hartree Fock (UHF) method was utilized for transition states suspected of high diradical character. The heats of formation and geometries of open shell radical products were calculated via the half-electron (HE) method.

THERMODYNAMIC CONSIDERATIONS

If the use of the 1-nitropropene molecule as a model for the TNT molecule has any validity, it is necessary that the two potential energy surfaces have the same topology. For example, the standard enthalpy changes associated with the six reactions studied should be similar in the two systems. The enthalpy changes are tabulated in Table 1 for calculations employing both the MNDO and MINDO/3 methods, together with the difference in ΔH^o for the propene system and the TNT system for a particular reaction. The data substantiates the validity of the model. In almost every case (the exception being the NO_2 group removal, calculated by the MINDO/3 method) the differences in ΔH^o for a given type of chemical pathway are relatively small, the difference being in the range of 0-12 kcal mol^{-1}. The MNDO model seems to provide the better degree of agreement for the two systems. The energetic order of the six steps is almost identical in TNT and 1-nitropropene; hence the model does exhibit about the same ordering of reactant and product states for both systems. This is an important point since it provides hope that the energetic order of the thermodynamic states of the model system parallel those of the TNT system.

CALCULATION OF TRANSITION STATES

Since the 1-nitropropene model does exhibit almost the same ordering of reactant and product states as TNT, it is reasonable to expect that 1-nitropropene reflects the proper ordering of all the energy maxima on the potential surface, thus enabling the identification and ordering of the transition states for the six reaction channels considered. Under this assumption, tentative reaction coordinates were identified for each of the six mechanisms and the transition states located, using both the MNDO and MINDO/3 methods. The transition states were identified by the method of Hildebrandt using the eigenvalues of the force constant matrix[8], i.e., by the presence of one, and only one, negative eigenvalue. The transition states so identified are diagrammed in Figures 2-6, where we illustrate their geometries and specify the bond orders. In Table 2 we list the enthalpy of activation for each of the six mechanisms, together with the frequency associated with motion along the reaction coordinate (normal coordinate basis). The latter was calculated by carrying out a Wilson-FG type of vibrational analysis for each transition state.[9] Since we cannot anticipate apriori which internal coordinates will enter a given normal coordinate and which combinations of these coordinates will in turn correspond to the translational and rotational motions, the latter have been left in the analysis. The frequencies calculated for translational and rotational motions never turned out to be identically zero but they were generally close to zero. In light of this, the frequencies calculated for motion along the reaction coordinate probably contain some error which we estimate could be as large as ±200 cm^{-1}.

Geometrically the transition states identified by the MNDO method and the MINDO/3 method were very similar. Since the parameterization for MNDO was done with no nitro-containing compounds[1] and a careful study of the accuracies of MNDO and MINDO/3 for nitro-containing *compounds has shown* MINDO/3 to be superior[10], we expect the MINDO/3 results to be more reliable.

The transition state obtained for the intramolecular hydrogen atom transfer of a hydrogen atom from the CH_3 end of the three carbon chain to the nitro group (Figure 2) is a cyclic structure wherein the hydrogen atom-carbon atom bond has been elongated from 1.10A to 1.34A (bond order of 0.42). The initial stages of O-H bond formation can be identified with the hydrogen oxygen distance of 1.17A (bond order of 0.44). The transition state is non-planar with the hydrogen being transferred about 0.5A out of the plane formed by the three carbon atoms.

The calculated activation enthalpy was somewhat higher for MNDO than MINDO/3 (63.7 kcal mol^{-1} compared to 43.4 kcal mol^{-1}). This is consistent with MNDO normally giving slightly high activation enthalpies for hydrogen transfer reactions. The MINDO/3 result is consistent with the experimental activation energy and thus this process cannot be ruled out as a first step in the thermochemical decomposition on the basis of this calculated activation energy. We would expect the TNT activation enthalpy to be several kcal mol^{-1} higher, however, because of the loss of the aromatic character of the ring as TNT converts to the product state. This effect, of course, will not show up in our 1-nitropropene model compound.

Now consider the transition state for the intermolecular hydrogen transfer. Since the product of this reaction is two radicals, the numbers given in Table 2 are for UHF-type wave functions. Attempts to optimize an RHF transition state resulted, as could be expected, in the separated reactants. In contrast to the intramolecular hydrogen transfer transition state, which was almost symmetrical in terms of the C-H and O-H bond orders, this intermolecular transition state shows that the C-H bond is more than half-broken (C-H distance is 1.36A, with a bond order of 0.30) while the O-H bond is more appreciably formed (O-H distance is 1.07A, with a bond order of 0.53).

Again, the calculated activation enthalpy for MNDO is somewhat higher than for MINDO/3 (50.4 kcal mol^{-1} vs. 39.6 kcal mol^{-1}), following the trend that MNDO overpredicts activation enthalpies for hydrogen transfer reactions. The MINDO/3 result for this reaction is also consistent with the experimental activation energy, although MINDO/3 UHF results typically may underestimate the activation enthalpy by several kcal mol^{-1}. Even so, the agreement with the experimental number is quite good.

In the MINDO/3 transition state for the intramolecular oxygen insertion from the nitro group into a C-H bond of the methyl group, the N-O bond is stretched (distance of 1.35A, bond order of 0.86), the C-H bond is stretched (distance of 1.25A, bond order of 0.59), the C-O bond is partially formed (distance of 1.63A, bond order of 0.29), and the O-H bond is partially formed (distance of 1.22A, bond order of 0.29). The geometry of the transition state is slightly non-planar, with the inserted oxygen atom and the hydrogen atom both about 0.1A out of the plane formed by the three carbon atoms.

There is a large difference between the calculated enthalpies of activation for MNDO and MINDO/3 (127.7 kcal mol^{-1} vs. 49.9 kcal mol^{-1}), even though the overall geometries are similar. Based on previously-discussed rationale, the MINDO/3 results are more believable. The MINDO/3 enthalpy of activation is slightly larger than the experimented activation energy, but the 10 kcal mol^{-1} difference does not completely rule this step out as a possible first step. We think, however, that it is less likely than the hydrogen transfer steps previously discussed.

In the MINDO/3-calculated transition state for the intermolecular oxygen insertion into a methyl group C-H bond, compared with the intramolecular insertion transition state, the reaction has proceeded more toward product. The N-O bond is stretched (distance of 1.38A, bond order of 0.75), the C-H bond is stretched (distance of 1.29A, bond order of 0.48), the C-O bond is partially formed (distance of 1.66A, bond order of 0.35), and the O-H bond is partially formed (distance of 1.11A, bond order of 0.39).

Like the intramolecular oxygen insertion, there is a large discrepancy between MNDO and MINDO/3 in the calculated enthalpies of activation for this intermolecular oxygen insertion (108.7 kcal mol^{-1} vs. 44.4 kcal mol^{-1}). Again, assuming the MINDO/3 value to be more accurate, this calculated activation enthalpy is consistent with the experimental activation energy. This process is quite likely to be taking place in the initial stages of TNT decomposition.

In the MINDO/3-calculated transition state for the nitro-nitrite rearrangement, one of the oxygens inserts into the C-N bond, resulting in the structure C-O-N-O. The transition state shows stretching of the C-N bond (distance of 1.45A, bond order of 0.71), stretching of the N-O partial double bond in the nitro group toward the single bond in the product (distance of 1.30A, bond order of 1.19), and partial formation of the C-O bond (distance of 1.53A, bond order of 0.45).

The results for the activation enthalpies are 35.0 kcal mol^{-1} and 51.6 kcal mol^{-1} for MINDO/3 and MNDO, respectively. Both values are not far removed from the experimental activation energy, making this process a feasible first step on an activation enthalpy basis.

The last process considered was a simple C-N bond fission, resulting in the C_3H_5 radical and NO_2. A reaction path calculation failed to produce a transition state, meaning that the reverse reaction should proceed without activation, a common occurrence for a radical recombination reaction. Thus, the activation enthalpy and the reaction enthalpy are one and the same. The results are 29.8 kcal mol^{-1} for MNDO and 41.4 kcal mol^{-1} for MINDO/3. Both values make the C-N bond fission look feasible when compared with the experimental activation energy, but we feel that both numbers are in error. MNDO results for heats of formation of nitroaromatics generally are far too endothermic,[10] destablizing the reactant and making the activation enthalpy too small. On the other hand, MINDO/3 gravely overstabilizes NO_2 by about 25 kcal mol^{-1}, again making the activation enthalpy too small. If one corrects the MINDO/3 result for this known error for NO_2, an activation enthalpy of about 65 kcal mol^{-1} is obtained. This number agrees with the 70 kcal mol^{-1} value one obtains for the C-N bond strength in nitrobenzene if the experimental heats of formation for nitrobenzene and NO_2, and the MNDO-calculated value for phenyl radical are used. This 70 kcal mol^{-1} value is also in the area of a C-N bond strength according to conventional organic chemistry wisdom. Thus, we feel that a simple C-N bond fission is <u>not</u> possible as a first step in the thermochemical decomposition of TNT.

CONCLUSIONS

Cis-1-nitropropene is a good theoretical model for studying TNT thermochemical decomposition. It reproduces all of the major structural features of a nitro group being ortho to the methyl group in TNT. Of all of the possible reaction steps we considered, only the intramolecular hydrogen transfer changes the aromaticity of the TNT system, making our 1-nitropropene model not quite as good for that case. Even so, we are able to deduce qualitative trends of this effect.

MINDO/3 results do appear to be more reliable than the MNDO results. We cannot explain the abnormally high values of the activation enthalpies that MNDO gives for the oxygen transfer steps. It is quite feasible that, in spite of repeated attempts, we have still not obtained the transition states for these processes with MNDO. In the other cases, the MINDO/3 and MNDO results are similar.

Our original goal was to draw conclusions about possible first steps of TNT thermochemical decomposition by comparing our theoretical results with the EPR and IDSC results. On an activation energy basis, several processes appear to be likely: both hydrogen transfers, both oxygen transfers, and the nitro-nitrite rearrangement. The fairly large isotope effect, however, is difficult to explain with anything but the two hydrogen transfer steps, although we are currently calculating deuterium isotope effects for all of these steps. The EPR signals indicate that radicals must be involved, and the spectrum shows two nitrogens and five hydrogens.

The intermolecular hydrogen transfer has the attraction that it produces radicals directly, but not with the required two nitrogens. HONO loss from the hydrogen transfer product does result in a radical with the required two nitrogens and five hydrogens, and further work is in progress to determine the feasibility of these follow-on steps.[11] On the other hand, intramolecular hydrogen transfer followed by OH loss would result in a radical, but with two nitrogens and only four hydrogens.

The intermolecular hydrogen transfer process is consistent with all of the known experimental facts for TNT thermochemical decomposition. Thus, we feel that it is a major process early in the decomposition. The low activation enthalpies calculated for several other steps, however, make it probable that these other processes go on just as well. Indeed, all of previous studies on TNT thermochemical decomposition indicate that the system is quite complicated, particularly in light of the multitude of intermediate products. Our calculations certainly indicate the complexity of the system.

References and Notes

(1) Dewar, M.J.S.; Thiel, W.; J. Am. Chem. Soc., 1977, 99, 4899; ibid. 1977, 99, 4907.

(2) Bingham, R.C.; Dewar, M.J.S.; Lo, D.H.; J. Am. Chem. Soc., 1975, 97, 1285.

(3) See Kollman, H.; Carrion, F.; Dewar, M.J.S.; Bingham, R.C., J. Am. Chem. Soc., 1981, 103, 5292. Oleksik, J.; Turner, A.G., Inorg. Chim Acta, 1982, 59, 165.

(4) Shackelford, S.A.; Beckmann, J.W.; Wilkes, J.S., J. Org. Chem., 1977, 42, 4201.

(5) Guidry, R.M.; Davis, L.P.; Thermochimica Acta, 1979, 32, 1.

(6) Carper, W.R.; Davis, L.P.; et. al., to be published.

(7) In any but the simplest of systems, the reaction coordinate cannot be identified apriori as any one of or linear combination of the members of an arbitrary set of internal coordinates. Methods for doing this are under investigation in this laboratory and others. A.G. Turner and C.E. Wulfman, to be published.

(8) Hildebrandt, R.L.; Comput. Chem., 1977, 1, 179.

(9) Wilson, E.B., Jr.; Decius, J.C.; Cross, P.C.; "Molecular Vibrations", McGraw-Hill Book Co., Inc. New York, 1955, Chapters 6-9.

(10) Guidry, R.M.; Davis, L.P.; Frank J. Seiler Research Laboratory Technical Report, to be published.

(11) Turner, A.G.; Davis, L.P.; J. Phys. Chem., to be published.

TABLE 1. STANDARD ENTHALPIES OF REACTION (kcal mol^{-1})

Reaction	MNDO			MINDO/3		
	1-Nitro-propene	TNT	Δ	1-Nitro-propene	TNT	Δ
Intra H Transfer	8.6	16	8.0	7.6	19.8	12.2
Inter H Transfer	16.2	16.8	0.6	38.2	38.7	0.5
Intra O Insertion	-49.5	-49.9	-0.4	-18.7	-18.4	0.3
Inter O Insertion	-51.3	-52.4	-1.1	-16.1	-21.9	-5.8
Nitro-Nitrite Rearrange-ment	-38.9	-41.1	-2.2	-7.5	-7.5	4.3
Nitro Group Removal	29.8	26.9	-2.9	41.4	62.1	20.7

TABLE 2. ACTIVATION PARAMETERS FOR 1-NITROPROPENE SYSTEM

Reaction	MNDO		MINDO/3	
	$\Delta H^{\ddagger}$ (kcal mol^{-1})	Frequency (cm^{-1})	$\Delta H^{\ddagger}$ (kcal mol^{-1})	Frequency (cm^{-1})
Intra H Transfer	63.7 (59.5)	2734 (3715)	43.4 (43.4)	1896 (1896)
Inter H Transfer	-- (50.4)	-- (3834)	-- (39.6)	-- (1701)
Intra O Insertion	127.7	1733	49.9	936
Inter O Insertion	108.7	1633	44.4	424
Nitro-Nitrite Rearrangement	51.6	1051	35.0	705

Nitro Group Removal	29.8	--	41.4	--

(   ) = UHF Calculation

Figure 1. The choice of cis-1-nitropropene as a theoretical model for TNT.

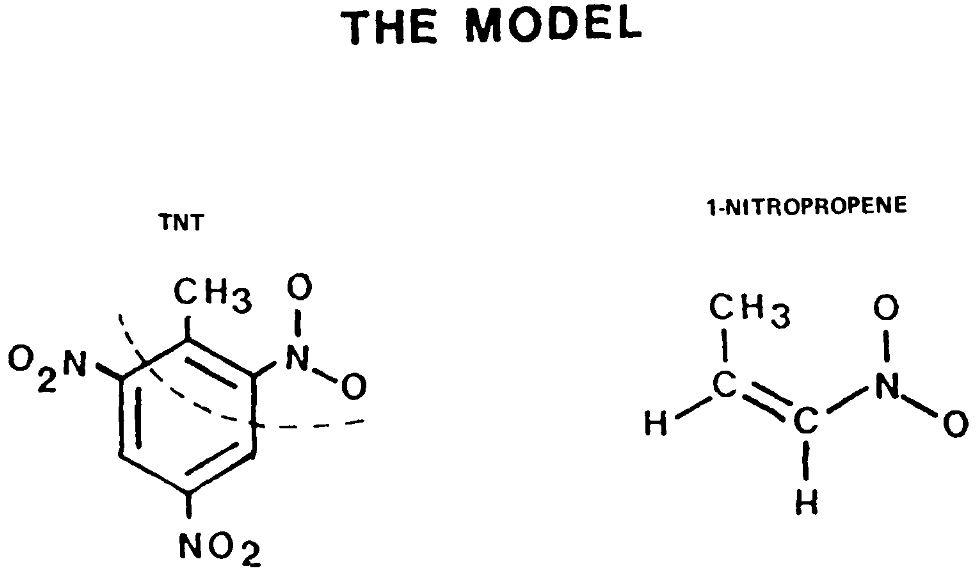

Figure 2. The MINDO/3-calculated transition state for the intramolecular hydrogen transfer. Numbers in brackets are bond orders. Unlabelled atoms are hydrogens.

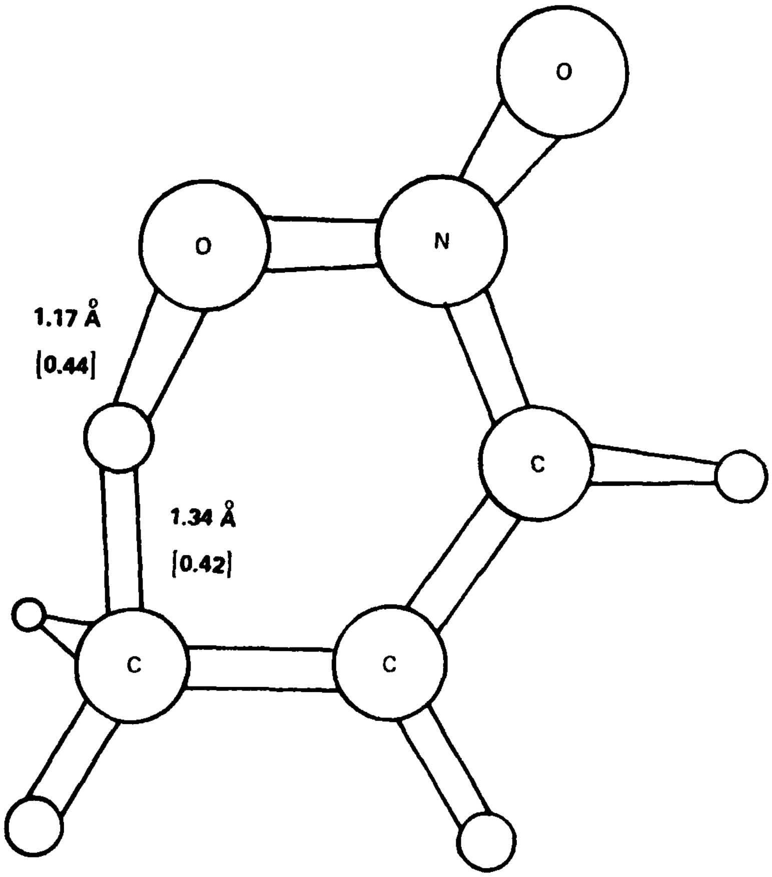

Figure 3. The MINDO/3-calculated transition state for the intermolecular hydrogen transfer. Numbers in brackets are bond orders. Unlabelled atoms are hydrogens.

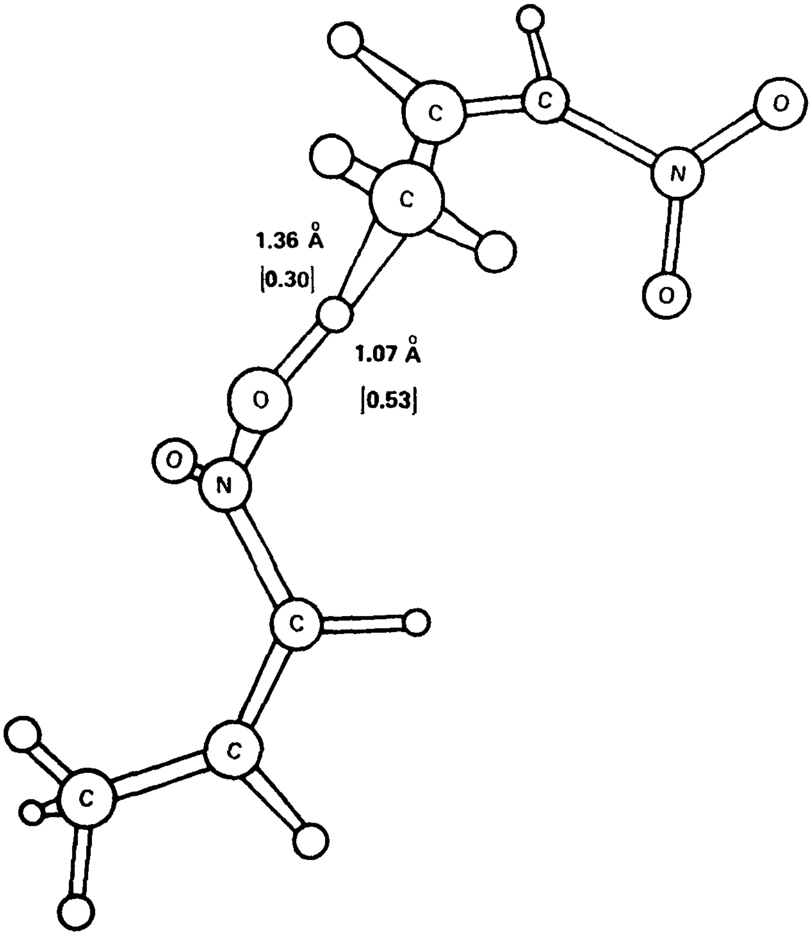

Figure 4. The MINDO/3-calculated transition state for the intramolecular oxygen insertion. Numbers in brackets are bond orders. Unlabelled atoms are hydrogens.

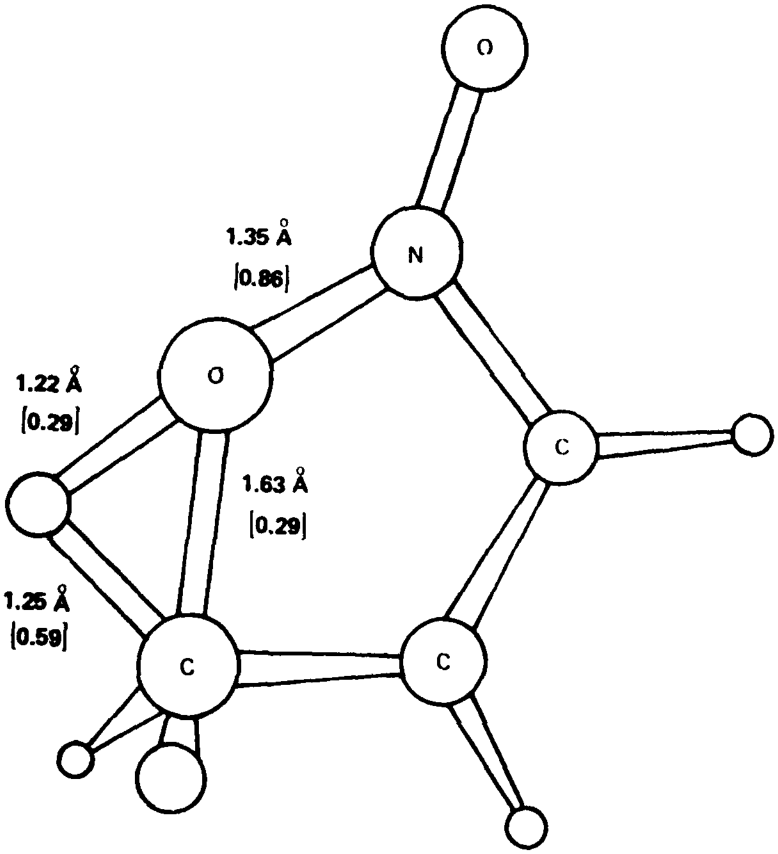

Figure 5. The MINDO/3-calculated transition state for the intermolecular oxygen insertion. Numbers in brackets are bond orders. Unlabelled atoms are hydrogens.

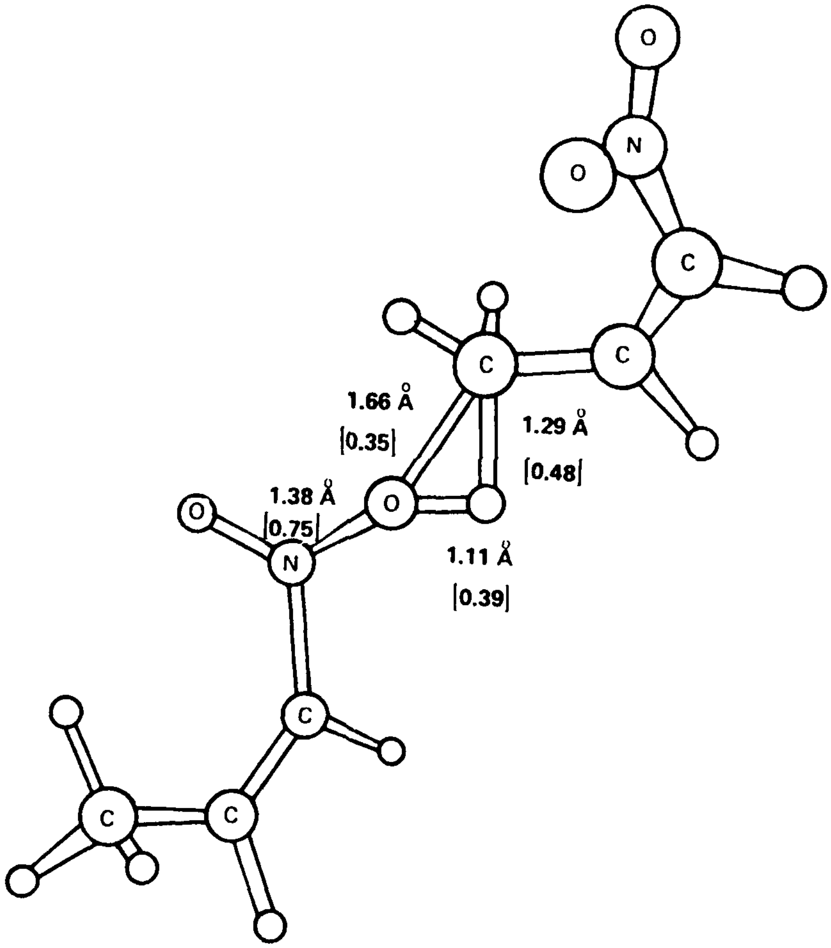

Figure 6. The MINDO/3-calculated transition state for the nitro-nitrite rearrangement. Numbers in brackets are bond orders. Unlabelled atoms are hydrogens.

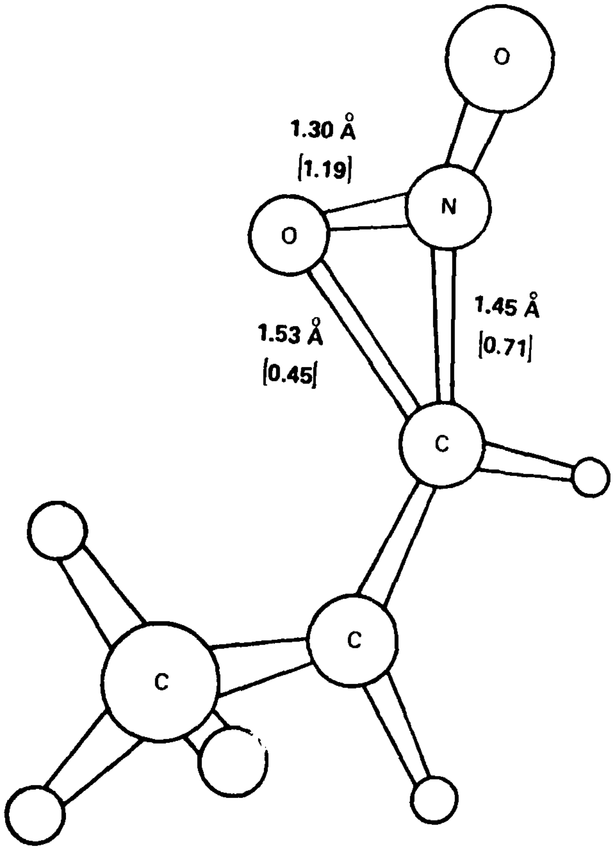

Chapter 5

ENERGETIC MATERIALS (TETRAZINE SYNTHESIS)

by Paul E. Vorndam

INTRODUCTION

Compounds with high nitrogen and oxygen and low hydrogen content can be desirable as energetic materials. Many compounds of this type have been synthesized, e.g., TNT, HMX, etc. A class of compounds which can also satisfy these energetic criteria but which has not, as yet, received extensive attention, are the tetrazines. Tetrazines have the general formula shown below:

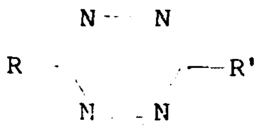

Air Force interest exists in the development of high energy materials to improve energy output, efficiency, shelf life, and economy of solid rocket propellants, munitions and high explosives for nuclear devices. Previous research in this area includes polynitroaromatic compounds such as pyrazoles, imidazoles, pyridines, picryls, etc. (See for instance references 1 and 2.) The goal of this research is to investigate the energetic properties of nitrated tetrazines via synthetic preparation.

EXPERIMENTAL PROCEDURE - Results and Discussion

TNT has long been a most useful explosive and therefore it was felt that TNT tetrazine analogs would be a logical starting point.

The target compounds are:

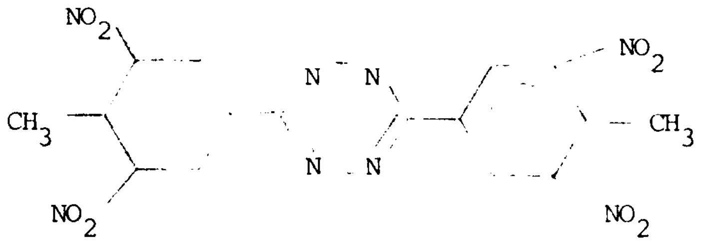

I

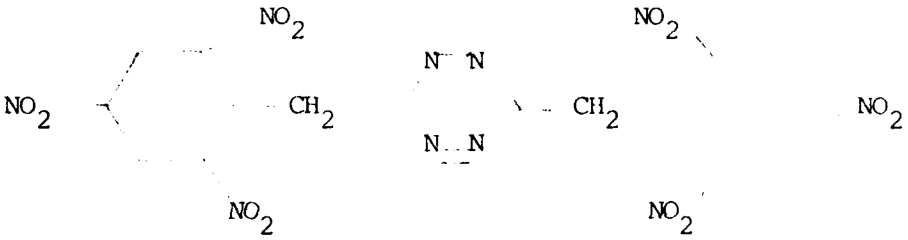

II

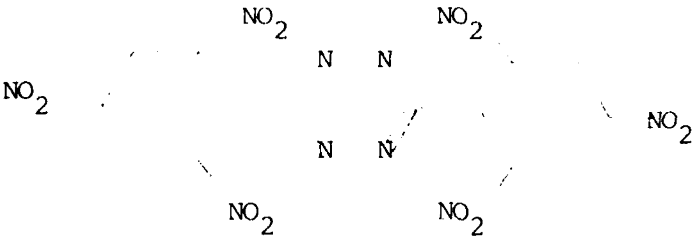

III

Compound I has been prepared and the mononitro analog of II has been prepared.

Although the synthesis reactions are straight forward, reaction yields have generally been below 50% for a given reaction. Reaction conditions have not been optimized, however. Compound III has not been synthesized yet. The tetrazine has been prepared in small quantities (< 500 mg). The *proposed route to III is:*

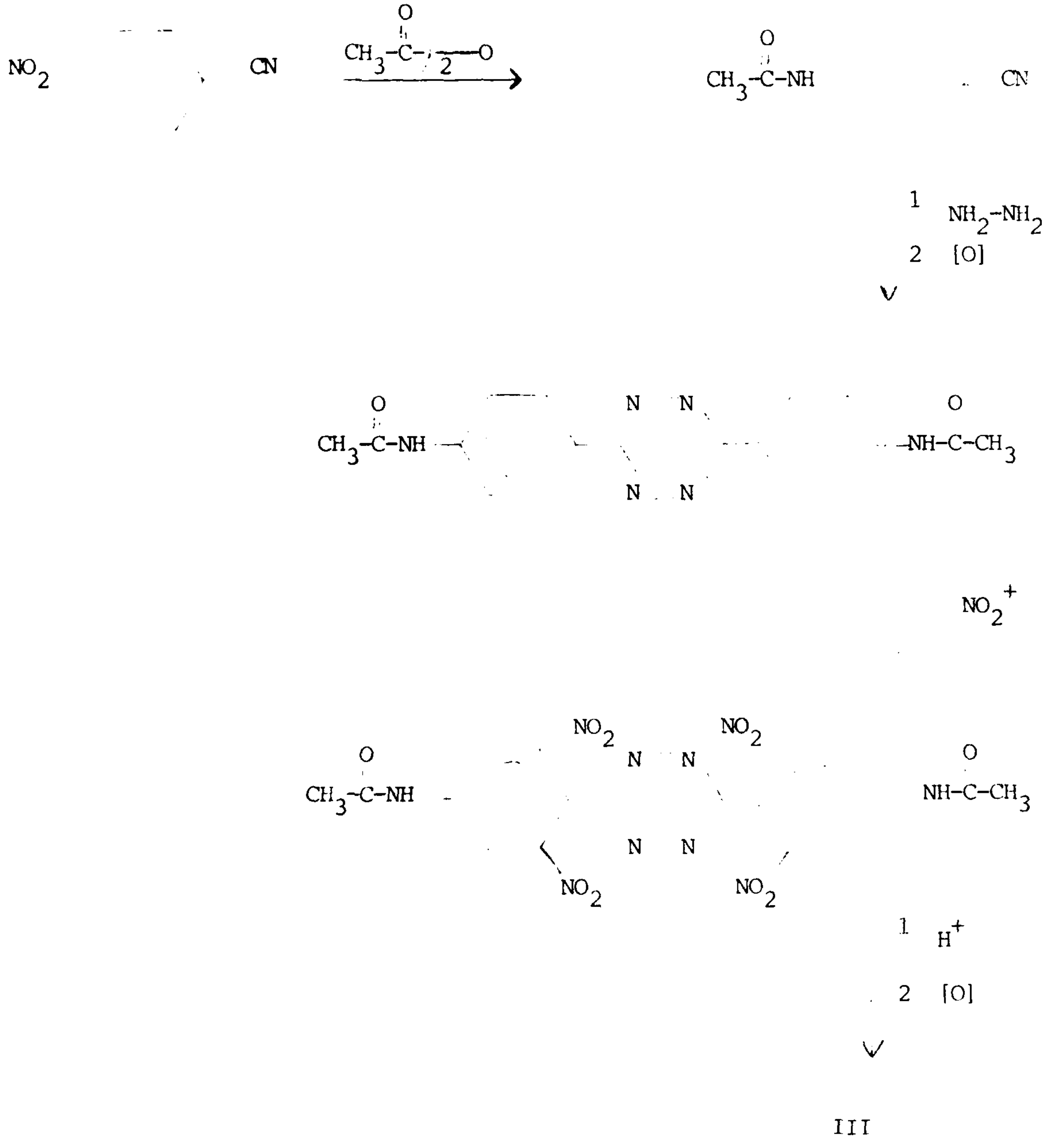

Recent results indicate that the last two steps to III will be difficult. A standard nitration of the acetylated tetrazine lead to degradation of the tetrazine ring and intractable tar. Future work on this compound should avoid oxidizing conditions while nitrating.

The non-acetylated tetrazine has been prepared (IV). Nitrations have not been attempted.

EXPERIMENTAL PROCEDURE

The tetrazine synthesis reactions are easily performed. Reaction conditions are usually mild. The synthesis is a two step process starting with aryl nitriles. In the first step an aryl nitrile is reacted with hydrazine to give a dihydrotetrazine:

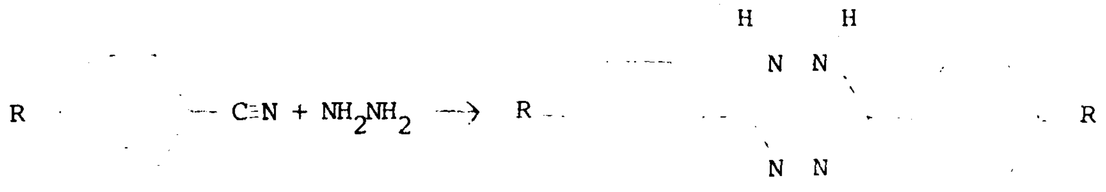

The dihydrotetrazine is then oxidized to the tetrazine:

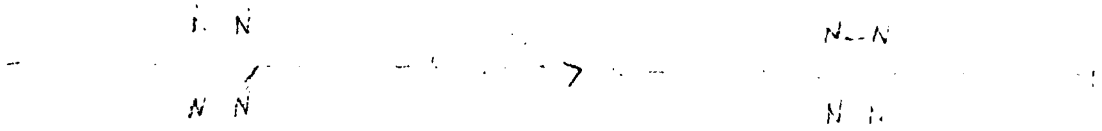

CONCLUSIONS

The results so far indicate that the nitrated tetrazines will probably not replace any current energetic material in use (due mainly to cost) but their use to augment current materials is still a possibility. Also, knowledge of the synthetic methods may be valuable with other materials.

REFERENCES

1. SYNTHESIS AND DECOMPOSITION OF NITRATED TETRAZINES, M.L. Druelinger, L.P. Davis, P.E. Vorndam, D.J. Easler, and L.A. Connell. Paper presented at ACSC Annual Meeting, Sep 1982.

2. Cady, H.H.; Coburn, M.D.; Harris, B.W.; Rogers, R.N.; Los Alamos Scientific Laboratory Informal Report LA-6802-MS, Synthesis and Thermochemistry of Ammonium 2.45 - Trinitroimidazole, Jul 1977.

Chapter 6

HETEROGENEOUS CATALYSIS

by Larry W. Burggraf, Ronald O. Klatt, and Larry P. Davis

ABSTRACT

The potential for immobilizing homogeneous catalyst analogs on solid supports prompted us to study the silylation reactions by which silica can be chemically modified with chelating functional groups. EPR spectrometry of copper (II) chelates suggests that oligomeric sites are stabilized on the surface. The ratio of multiple interaction sites to isolated sites is insensitive to surface coverage. MNDO calculations on neutral and anionic silanol polymers has begun. Preliminary calculations show that 5-coordinate bridge structures are especially stable.

INTRODUCTION

For many practical reasons, all ultimately related to cost, heterogeneous catalysts are the mainstay of chemical industry. However, homogeneous catalyst have shown advantages which can not be ignored; particularly high selectivity, more moderate reaction conditions, specific known active centers, asymmetric induction and better control of catalytic properties through chemical manipulation of active centers.[1] As a result, a great deal of attention has been recently devoted to hybrid catalyst in which known homogeneous catalyst are "heterogenized" by immobilizing them on solid supports. Often, because homogeneous processes are more readily studied, the homogeneous catalysis mechanism of interest is well characterized.

since there is no evidence for significant differences in mechanisms of homogeneous and heterogeneous catalysis, the transfer of active centers from homogeneous solution to surfaces of solid supports seems to be a logical approach for producing practical new industrial catalysts. These hybrid catalysts offer the promise of better temperature stability, a wider selection of solvents, in addition to the effect of the immobile active centers which may be advantageous or detrimental depending on the catalytic mechanism. See the book "Catalysis by Supported Complexes" by Yermakov, Kuznetsov and Zakharov[1] for a discussion of differences in catalytic activity produced by anchoring the active center on a solid support.

Inorganic oxides, especially silica, are frequently used as support surfaces because of their rugged physical properties and relatively low cost. Additionally, functional groups may be easily attached to these surfaces by reaction with surface hydroxyl sites. For example, organic functional groups can be immobilized by reactions of trialkoxysilanes (siloxanes) or trichlorosilanes with silica surface silanols as shown in Figure 1.

Figure 1. Silylation chemistry.

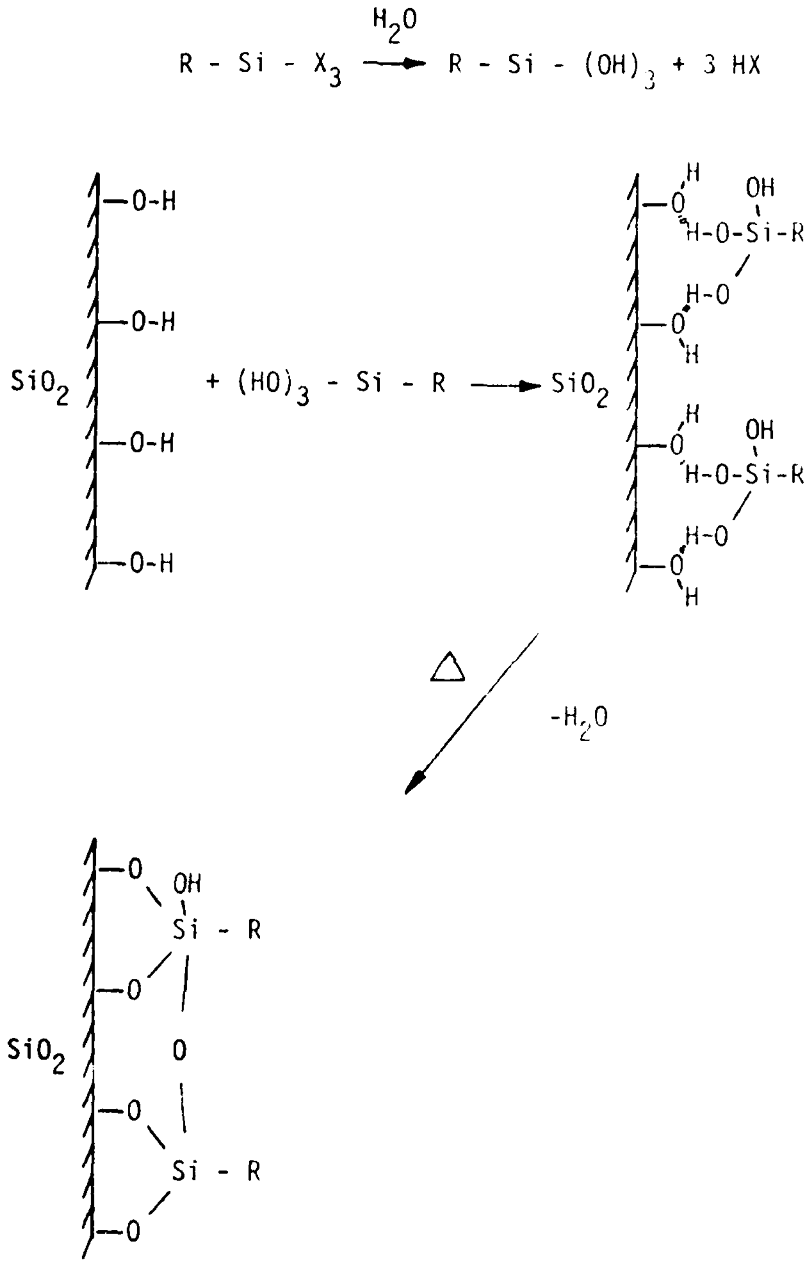

$$R - Si - X_3 \xrightarrow{H_2O} R - Si - (OH)_3 + 3\ HX$$

$X = OCH_3,\ OCH_2CH_3,\ Cl$

This chemistry for chemically modifying surfaces has also been applied to preparation of bonded phase chromatography materials, immobilization of enzyme catalysts and biological materials, and many other uses. For a discussion of these applications see the article "Tailoring Surfaces with Silanes" by Barry Arkles.[2]

An example of a hybrid catalyst prepared using this method is the catalysis of hydrogenation, hydrosilylation and hydroformylation of olefins by immobilized rhodium complexes prepared by silylation of silica.[3]

$$=\mathrm{Si{-}OH} + \mathrm{(EtO)_3SiCH_2CH_2PPh_2Rh(acac)(CO)} \xrightarrow{-\mathrm{EtOH}} \equiv\mathrm{Si{-}O{-}Si{-}CH_2CH_2PPh_2Rh(acac)(C}$$

A more general method is to immobilize a chelating ligand by silylation, or a functional group which is subsequently converted into a chelating ligand, and then anchor the active complex to that ligand. With this method it is more difficult to ensure that a single type of site has been produced on the surface.

In either case, the distribution of sites on the surface depends on many experimental factors. The density of silanols depends on the preparation of the silica and on the extend of dehydration of the silica surface. The extent of reaction depends not only on the silica surface but also on the silane reactivity ($=\mathrm{Si{-}Cl} > =\mathrm{Si{-}OCH_3} > =\mathrm{Si{-}OC_2H_5}$) and the silylation conditions, especially solvent and temperature. The distribution of sites on the surface is especially important for catalysis by supported metal complexes because the catalytic activity of a metal complex especially depends on the nature and degree of coordination sphere saturation.

In previous work[4] we have shown that at least two types of sites can be generated when a silica surface is silylated. The immobilized ligands are either close enough on the surface to chemically interact with a near neighbor or they behave as though they are chemically isolated. An immobilized ethylenediamine ligand, AEAPS:

(N-(2-aminoethyl)-3-aminopropyltrimethoxysilane derivatized silica gel)

on silica was shown to have sites capable of bonding Cu(II) ions in a mono complex while others bound the Cu(II) in a bis complex, illustrated in Figure 2. Previous work by Pinnavaia et al[5] using E.P.R. to monitor the nature of the immobilized Cu(II)-ethylenediamine complex produced a similar mono-to-bis site ratio even though the density of surface coverage was an order of magnitude smaller.

Figure 2. Copper (II) addition to bis binding site.

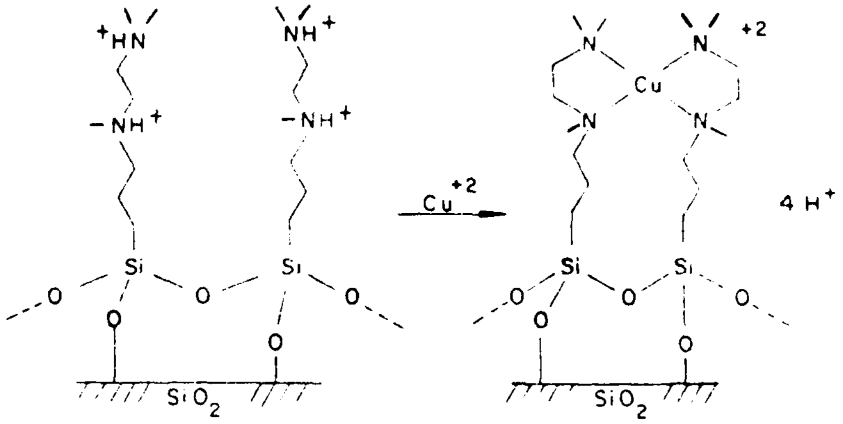

This suggests that oligomeric "clumps" of silane are stabilized on the surface template which induces oligomer stability or because the chemistry of silylation produces oligomers. Other evidence has prompted this suggestion by Kuznetsov[6], Waddell et al[7], and Lochmuller et al[8]. C.H. Lochmuller et al[9] recently used fluorescence of immobilized pyrene monomer and bimolecular excimer to study surface distribution of immobilized silane on silica. They conclude that there are high density regions in which pyrene rings are less than 4.5A apart and low density regions where the average distance exceeds 8A.

There are two areas in which we have begun to make contributions toward the ultimate objective of this research: to find methods for synthesis of chemically modified surfaces with well-characterized surface sites which may be evaluated for catalytic activity. First, the MNDO program was applied to the study of silanol polymerization reactions. This chemistry is important not only because it is the basis of silylation reactions which are used to modify the surface, but also because the amorphous silica surface itself is built up by silanol polymerization. This modeling tool can help us to understand the nature of the silica surface and the interactions of molecules with this surface. Eventually MNDO should permit us to model active centers which preferentially selects the configuration of the reactant molecules transition state, analogus to the lock-and-key model for enzyme active sites. The second area in which work has begun is synthesis of isolated surface monomers.

We performed a beginning experiment designed to isolate ligands on the surface by diluting chelating siloxanes with nonchelating siloxanes. Future work will modify this approach by using templates adsorbed onto the surface. Both of these areas of work will be discussed in the Results and Discussion section.

Experimental

A. Continuous Variation Study.

A continuous variation study was performed with aqueous solutions of the AEAPS silane and Cu^{2+} ions using EPR much as had been done previously using absorption spectroscopy.[4] This experiment was performed to confirm that we could distinguish between mono and bis copper complexes using EPR. The total concentration of chelate and $copper^{2+}$ was 5.0×10^{-3}M for ten solutions having varying ratios of metal ion and AEAPS silane. These solutions were studied in thin cells using EPR spectrometry.

B. Preparation of Surfaces.

The chelating siloxane used throughout this study was N-(2-aminoethyl)-3-aminopropyltrimethoxy silane (Petrarch Z-6020), hereafter designated AEAPS. This material was vacuum distilled before use. The nonchelating silane used in this study was trimethylchlorosilane (Aldrich), designated TMCS. The silanes were immobilized on silica gel (Baker chromatography grade 40-140 mesh) which had been dried overnight in a vacuum oven at 80°C. Solutions (5% V/V) of the silanes were prepared in dry methanol. These solutions were mixed to give chelating silane (AEAPS) mole fractions of 1.0, 0.7, 0.5 and 0.2 relative to the nonchelating silane (TMCS). Samples of the silica gel (2.0 grams) were stirred with 30 mL of the silane mixtures for six hours at room temperature. Each sample was filtered and washed with methanol. The silylated silica gel samples were cured in a vacuum oven at 80°C for 12 hours. As expected, the samples which had been silylated with trimethylchlorosilane were found to be hydrophobic. These surfaces were wetted with methanol before they were equilibrated with copper (II) solution. Samples of the silylated silica gel weighing 0.20 g were equilibrated with 30 mL of 1.0 x 10^{-2}M copper (II) nitrate buffered to pH 5 with 0.10 M acetate buffer. After 30 minutes the silica gel was separated by filtration, washed with deionized water and dried. These materials were also studied using EPR spectrometry.

C. EPR Spectrometry.

The EPR spectrometer used in this work was a Varian Model E-109E Spectrometer. Typical instrument parameters were.

	Aqueous Solution	Silica Gel
Microwave Frequency	9.095 - 9.098 GHZ	9.0998 - 9.1050 GHZ
Microwave Power	0.50 mW	1.0 mW
Modulation Frequency	100 KHZ	100 KHZ
Modulation Amplitude	20 G	20 G

RESULTS AND DISCUSSION

A. Experimental Results

(1) Continuous Variation Study

In Figure 3 EPR signals are shown are for 0.5:0.5 aqueous Cu^{2+} metal ion-to-ligand molar ratio and 0.4:0.6 molar ratio. At equal molar concentrations of metal ion and ligand the mono complex predominates in solution. The mono spectrum is a quartet with lines as 3147, 3079, 3008, and 2947 G at 9.0949 GHZ. At lower metal ion-to-ligand mole ratio a peak attributable to the bis complex begins to grow in at higher field.

Figure 3. EPR Signals: Aqueous Solutions of Cu^{2+} and Siloxane Ligand

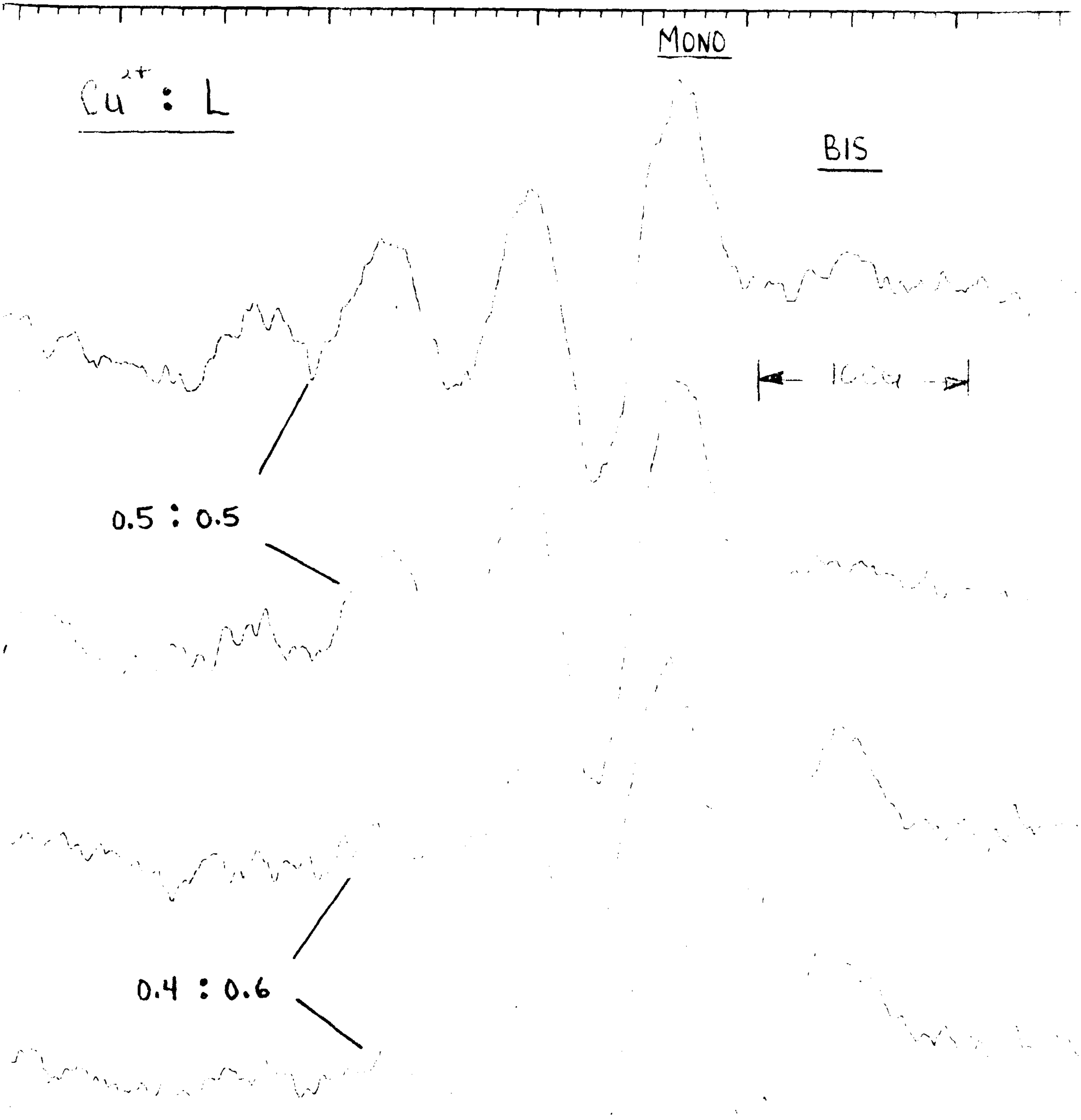

Figure 4. EPR Signals: Aqueous Solutions of Cu^{2+} and Siloxane Ligand

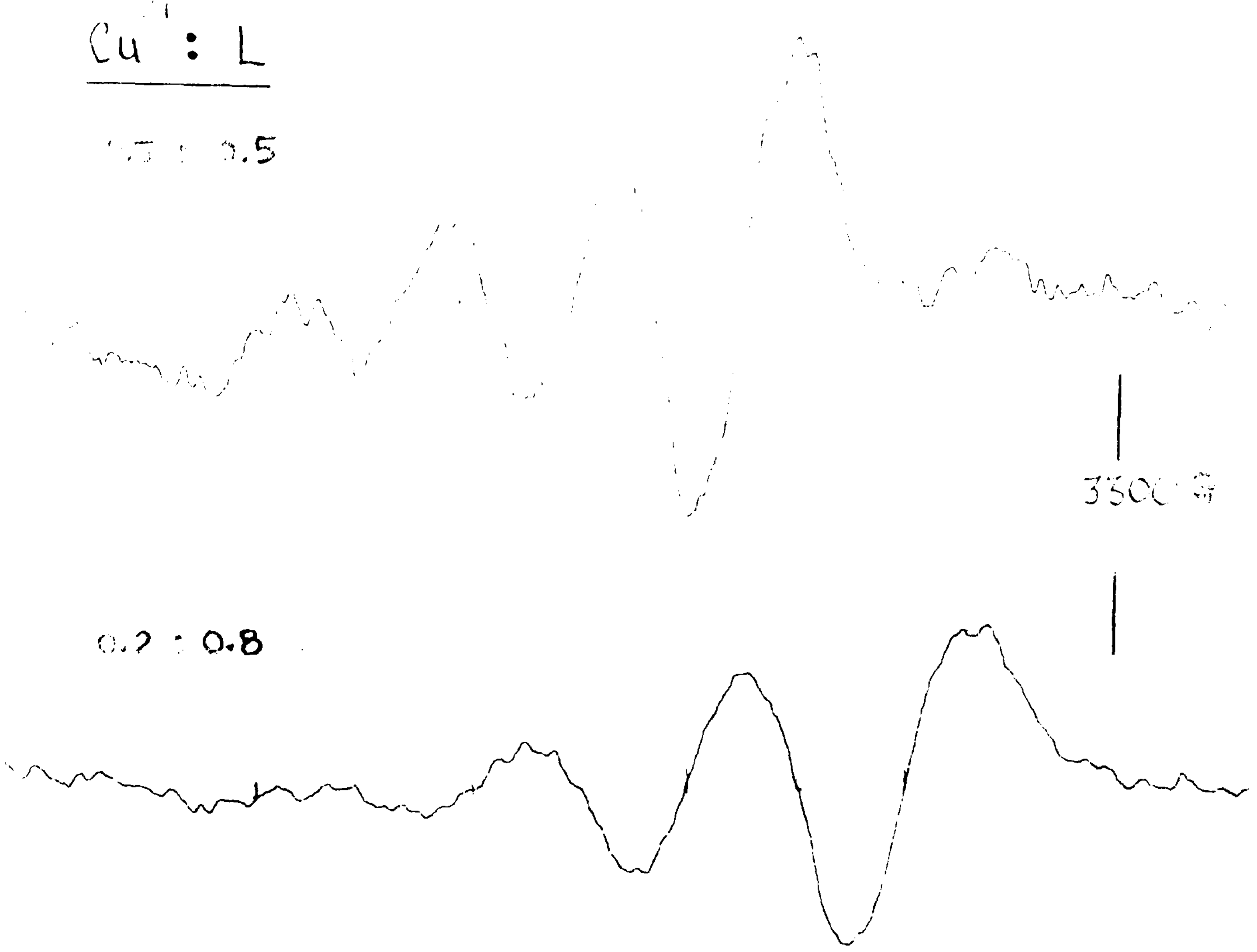

At 0.2:0.8 molar ratio the bis species dominates in solution. The EPR spectrum for this solution is shown in Figure 4. The bis spectrum is a quartet with lines at 3217, 3130, 3042, and 3156 at 9.0949 GHZ. In this way we may distinguish between the mono and bis contributions. The intensity corresponding to the bis complex is measured at ~3240 G and the intensity corresponding to the mono complex at ~3180 G producing the continuous variations plot shown in Figure 5. The continuous variation plot is in agreement with our spectral assignments.

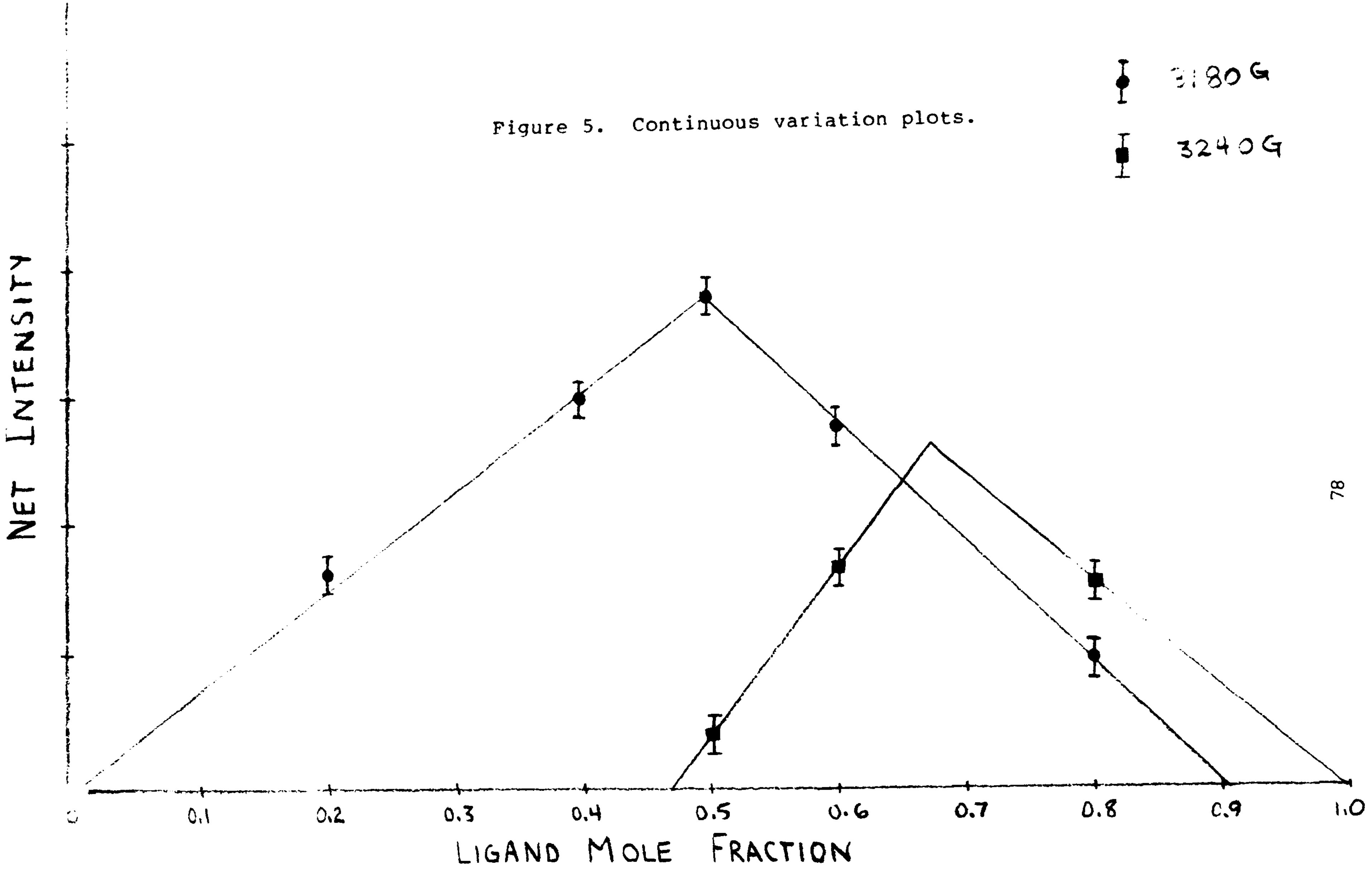

Figure 5. Continuous variation plots.

(2) Surface Immobilized Complexes

The EPR spectra of immobilized complexes resembled a dominant singlet with a superimposed quartet as shown in Figure 6. This spectrum was observed when pH was adjusted with acetate buffer or with ammonium buffer. The singlet component dominated the spectrum. This signal resembled very much the singlet signal of aqueous copper (II) nitrate. We identify this singlet signal with multiple (bis) coordinating ligand sites on the surface. We associate the quartet with the mono coordinating sites on the surface.

Figure 6. EPR spectra of copper (II) complexes on silica surface; ph = 6 using ammonium buffer.

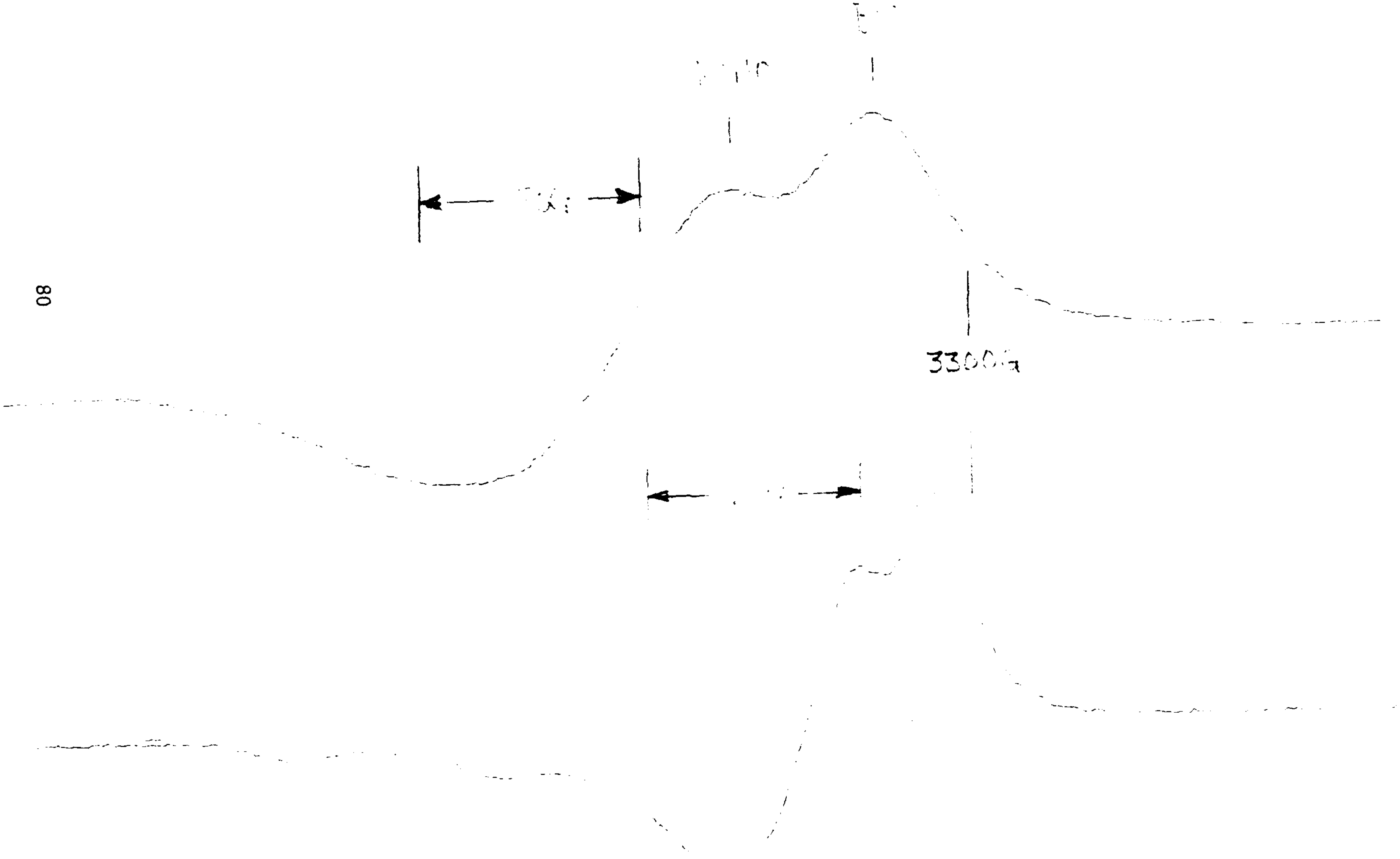

Figure 7 shows the mono-to-bis intensity ratio for the surfaces prepared with diminishing AEAPS loading. Figure 8 shows the corresponding intensity of the mono complex signal with diminishing AEAPS loading. While the surface coverage of chelating sites decreases by seventy percent there is no substantial change in the type of Cu^{2+} binding. If indeed oligomers of the trisiloxanes are stabilized on the surface we would expect a single AEAPS site surrounded by n other sites capable of interacting to multiply bind the copper (II) ion as dictated by the thermodynamics of the situation.

Figure 7. Plot of mono-to-bis EPR intensity ratio versus AEAPS mole fraction.

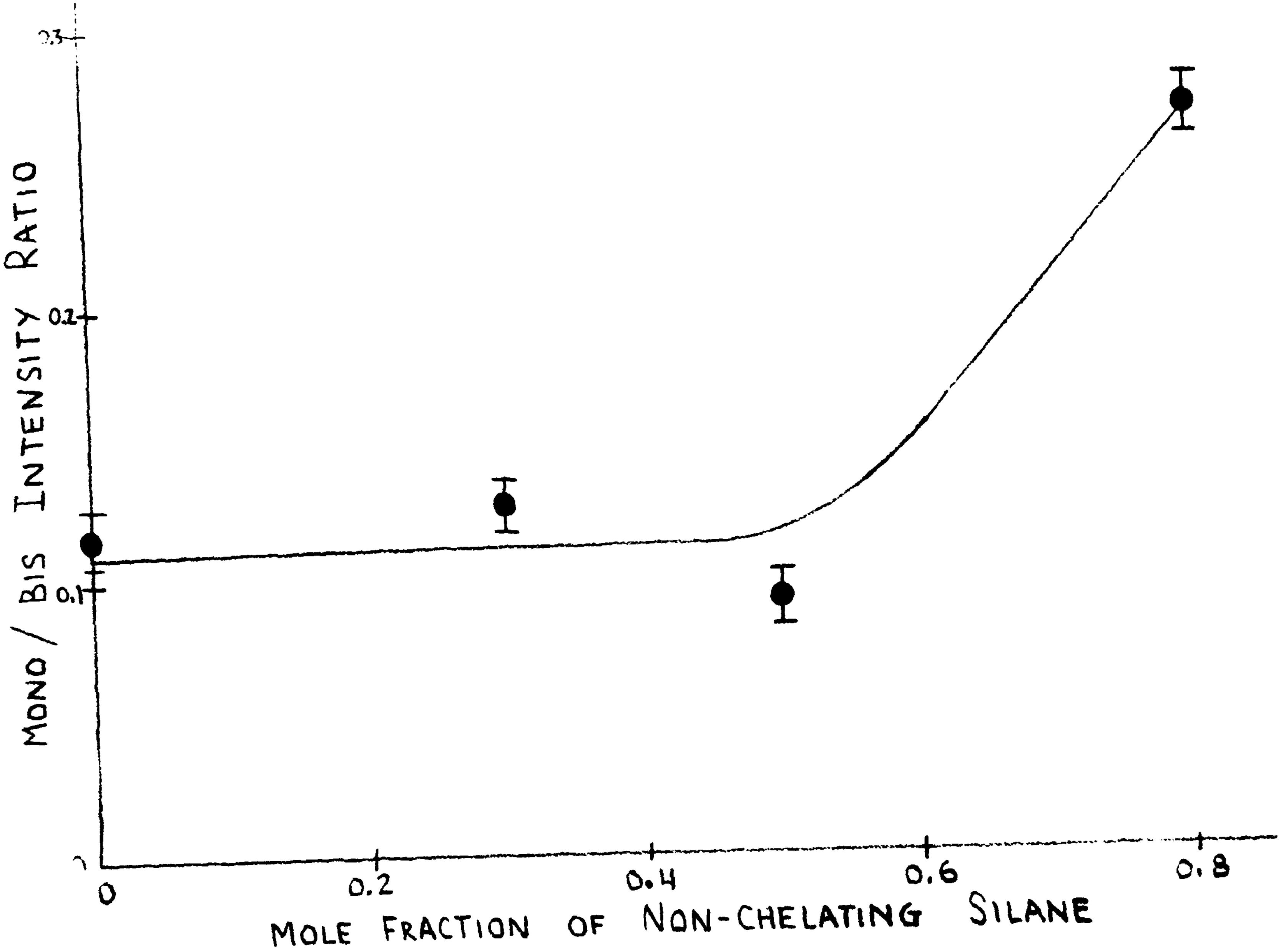

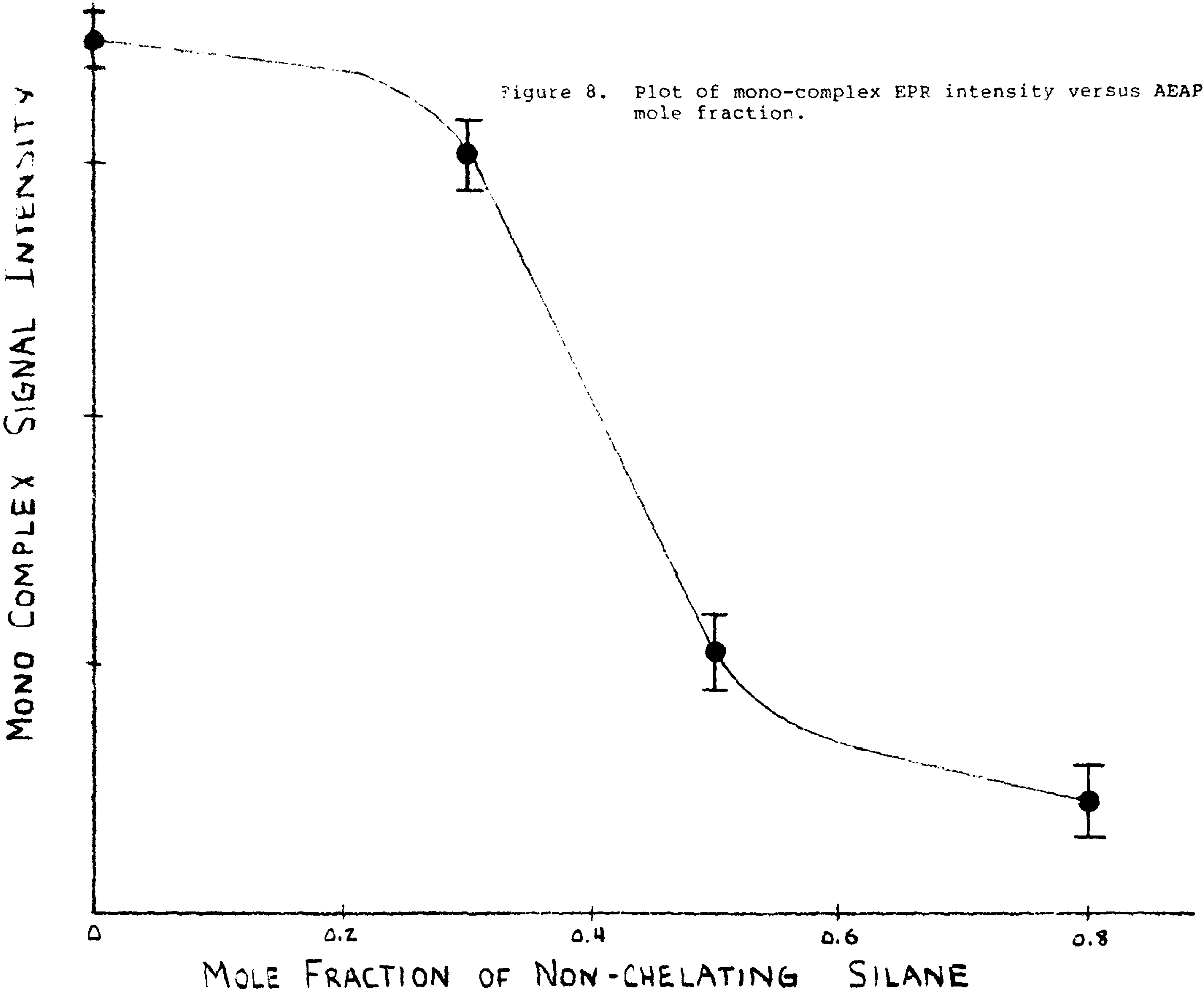

Figure 8. Plot of mono-complex EPR intensity versus AEAPS mole fraction.

Only when the number of interacting neighbors is reduced to less than 1/n will the average binding of the metal ion be affected. Based on this model our data suggests that $3<n<4$, i.e., oligomeric clumps of up to four or five interacting molecules are formed. These molecules may or may not be bound together. However, the results indicate that an immobilized chelating ligand may stretch to interact with 3.5 neighbors on average. It is interesting to note that the half-width of the multiply binding ("bis") signal in Figure 9 behaves very much like our measure of the surface coverage, the mono signal intensity. This fits the model well if the line narrowing is due to diminished spin-spin coupling as Cu^{2+} ions are removed from the oligomeric site. This is not conclusively established. A diminished contribution from a mono species to this line would also produce this trend.

Figure 9. Plot of bis-complex EPR line width versus AEAPS mole fraction.

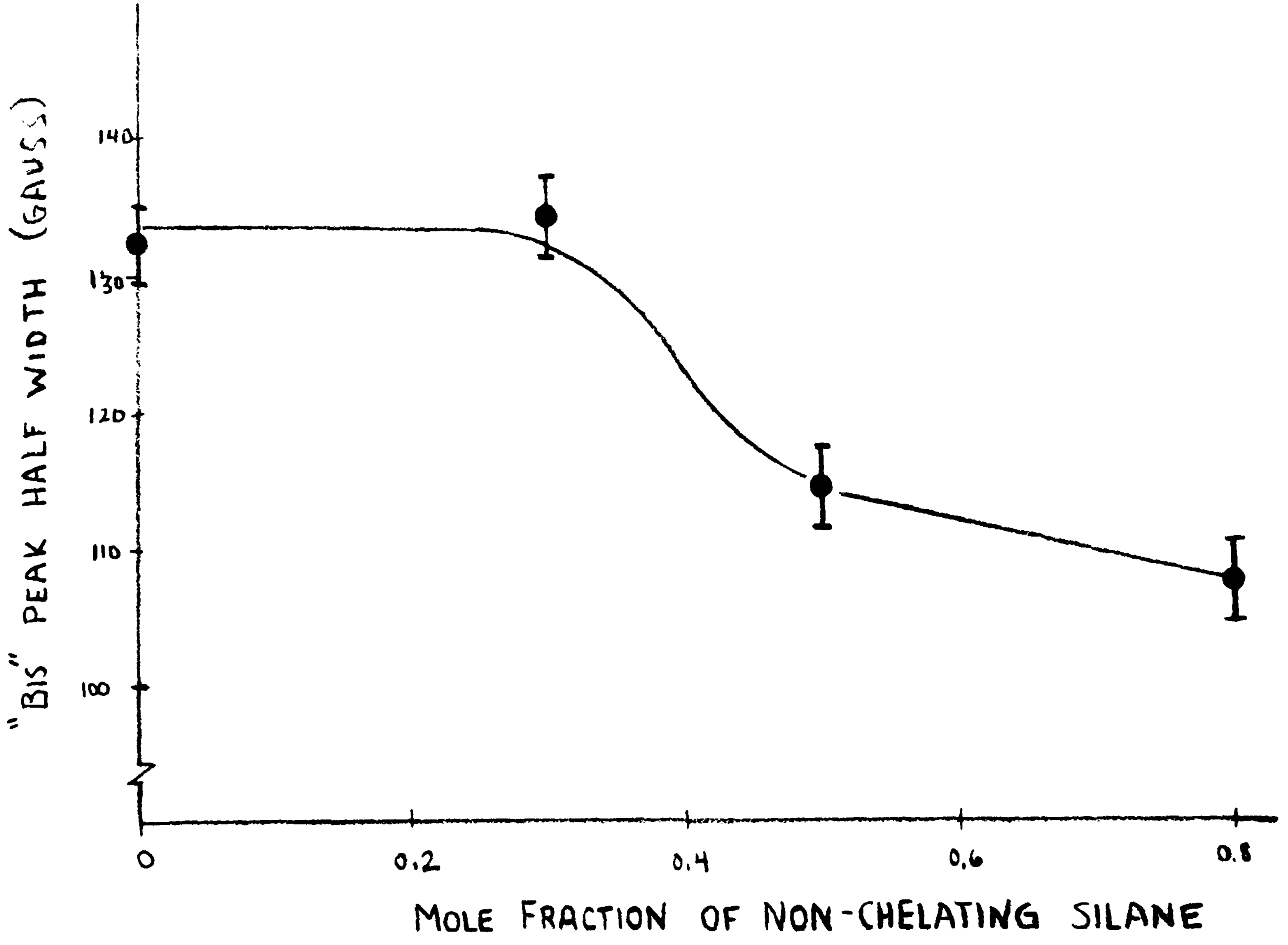

B. MNDO Calculations

In order to better understand the nature of the silica surface and the silanol condensation reactions employed to chemically modify these surfaces we began a study of silanol condensation reactions. Our aim is to correlate these calculations with what is known from studies of siloxane and SiO_2 polymerization.[10]

The rate of silica polymerization is a minimum at pH 2. At higher pH the polymerization is base-catalyzed and at lower pH it is acid-catalyzed. The mechanisms proposed for this polymerization have involved expanded coordination for silicon. Six-coordinate silicon has been an especially favored hypothesis.[10] Some sort of rearrangement then occurs which ultimately leads to the elimination of water. The net reaction is known to be essentially athermic. The activation energy in acid is 24 kcal/mole and in base 16.1 kcal/mole.

To attack this problem we started by investigating the base catalyzed mechanism. We began by optimizing larger and larger polymeric neutral and anionic silanol structures. While this work isn´t yet complete several points are becoming clear. First of all, the MNDO calculations have shown that bridging structures involving a 5-coordinate silicon have a special stability. The dimer is especially stable. This correlates well with an induction period known to occur in polymerization of monomeric silica.[10] However elimination of water from these species requires too much energy. So, the search for an energetically reasonable reaction intermediate continues.

FUTURE WORK

1. Experimental

Our next objective is to synthesize a specific type of chelating site on the silica surface. This will be done by first putting a template molecule on the silica surface. This idea takes advantage of the affinity of amines for dicarboxylic acids. HO_2C-R-CO_2H. Such a surface treated with the amine siloxane should preferentially take on a configuration dependent on R. The objective is to make an R-sized site on the silica surface. Each step of this synthesis can be followed by IR and UV spectroscopies as well as characterizing the end product using spectrometry.

References

1. Yermakov, Yu.I.; Kuznetsov, B.N.; Zakharov, V.A. "Catalysis by Supported Complexes", Studies in Surface Science and Catalysis, Volume 8; Elseoier: New York, 1981; Chapter 1.

2. Arkles, Barry; Chemtech, 1977, 7, 766-778.

3. Capka, M.; Svoboda, P.; Cerny, M.; Hetflejs, J.; Tetrahedron Letters, 1971, 50, 4787-4790.

4. Burggraf, L.W.; Kendall, D.S.; Leyden, D.E.; Pern, F. J., Analytica Chimica Acta, 1981, 129, 19-27.

5. Pinnavaia, T.J.; Lee, J.G.; Abedeni, M. In "Silylated Surfaces"; Leyden, D.E.; Collins, W., Eds.; Gordon and Breach: New York, 1980, Vol. 8, p. 333.

6. Kuznetsov, V.L., "Synthesis and Catalytic Properties of Complexes of Palladium and Cobalt on Silica," Ph.D. Thesis: Institute of Catalysis, Novosibirsk, 1977.

7. Waddell, T.G.; Leyden, D.E.; DeBello, M., J. Am. Chem. Soc., 1981, 103.

8. Lochmuller, C.H.; Wilder, D.R., J. Chromatog. Sci. 1979, 17, 574.

9. Lochmuller, C.H.; Colborn, A.S.; Hunnicutt, M.L., Anal. Chem., 1983, 55 1344-1348.

10. Iler, R.K., "The Chemistry of Silica", John Wiley: New York, 1979. Chapter 3.

Chapter 7

Synthesis of Metallametallocenes

by Hans J. Mueh and Silvia A. Beatty

ABSTRACT

Reaction of thiophene with $Fe_3(CO)_{12}$ has been shown to produce $Fe(CO)_3C_4H_4Fe(CO)_3$. Further treatment with $C_5H_5Co(CO)_2$ yields the ferracobaltocene species $C_5H_5CoC_4H_4Fe(CO)_3$. This project was an attempt to synthesize and examine that compound and the isostructural species $C_5H_5FeC_4H_4Fe(CO)_3$ and $C_5H_5NiC_4H_4Fe(CO)_3$. The species were to be studied in an attempt to determine the effect on the carbonyl stretching frequencies and variation of the electron density around the metal center using infrared spectroscopy for the former and cyclic voltammetry for the latter. Successful syntheses have yet to be developed for the compounds.

THEORY

The metallametallocenes are a recent off-shoot of the class of synthetic compounds known as metallocenes. The first metallocene to be synthesized and characterized was the stable orange compound biscyclopentadienyliron(II) or ferrocene, shown below.

Ferrocene

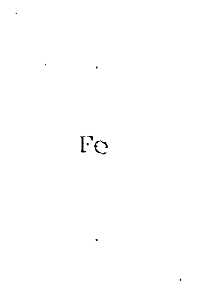

AD-A141 015 UNITED STATES AIR FORCE ACADEMY DEPARTMENT OF CHEMISTRY 2/2
RESEARCH: AY 1982-83(U) AIR FORCE ACADEMY CO
L P DAVIS ET AL. MAR 84 USAFA-TR-84-6

UNCLASSIFIED F/G 7/4 NL

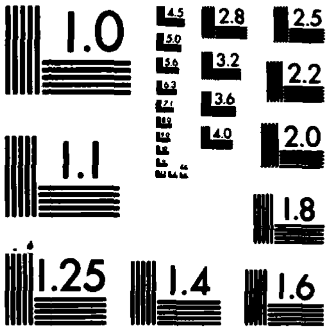

MICROCOPY RESOLUTION TEST CHART
NATIONAL BUREAU OF STANDARDS-1963-A

Ferrocene was the first known compound in which a metal atom was bound aromatically to carbon rings.

A good indicator of the feasibility and stability of an organometallic compound is the Effective Atomic Number (EAN) Rule[1]. This rule basically states that compounds in which the valence shell of the metal is filled are more likely to exist and to be stable. For the first row transition metals the valence shell consists of the 4s, 4p, and 3d orbitals. For the first row transition metals 18 electrons are needed to fill the valence shell, providing stability.

Ferrocene obeys the 18 electron rule as shown in the example below.

Ferrocene		Electrons Contributed to Valence Shell
Fe		8
$2C_5H_5^{\cdot}$	2x5	10
		18

The compound $C_5H_5CoC_4H_4Fe(CO)_3$ also obeys the 18 electron rule as shown below.

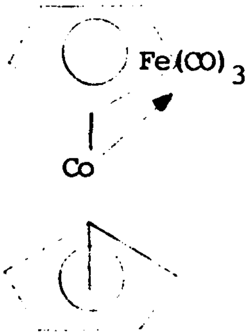

For Co		
Co		9 e^-
C_5H_5		5 e^-
C_4H_4		4 e^-
Fe		1 e^-
		19 e

For Fe		
Fe		8 e^-
3CO	3x2	6 e^-
2CH	2x1	2 e^-
Co		1 e^-
		17 e
TOTAL		36 e^-

However, in order to obey the 18 electron rule the cobalt must donate one electron to the iron so that the rule is obeyed for both transition metals. In order to obey the electron rule $C_5H_5FeC_4H_4Fe(CO)_3$ is expected to exist as an anion and $C_5H_5NiC_4H_4Fe(CO)_3$ as a cation. This may not be the case since metallocenes do not always obey the 18 electron rule. The neutral species of cobaltocene and nickelocene have both been isolated. However, these species are not stable. Cobaltocene, with 19 valence electrons, readily oxidizes to the cation. Therefore, the species $C_5H_5FeC_4H_4Fe(CO)_3$ and $C_5H_5NiC_4H_4Fe(CO)_3$ are expected to exist as ions.

EXPERIMENTAL

Synthesis of Ferrocene

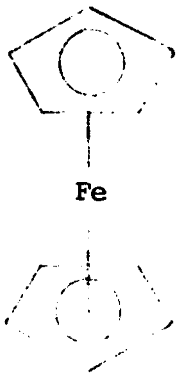

Purpose. Ferrocene was synthesized to provide experience in inorganic synthesis techniques like the use of nitrogen lines and to provide experience in handling typical inorganic reagents.

Procedure. The basic procedure used for the synthesis of ferrocene was that given in Jolly[2]. The overall reaction was:

$$11KOH + 2C_5H_6 + FeSO_4\ 7H_2O \longrightarrow Fe(C_5H_5)_2 + K_2SO_4 + 9KOH\ H_2O$$

Cyclopentadiene was prepared by cracking dicyclopentadiene by distillation through a fractionating column. A magnetic stirring bar, 120 ml of 1,2-dimethoxyethane, and 50 g of powdered potassium hydroxide were placed in the three-necked flask. While the mixture was stirred and the flask was flushed with a stream of nitrogen, 10.5 ml of cyclopentadiene were added. A solution of 18.2 g of $FeSO_4 \cdot 7H_2O$ in 50 ml of dimethyl sulfoxide was placed in the pressure-equalizing dropping funnel and added dropwise over a period of 20 minutes. The resulting solution was stirred for 30 minutes and was then added to a mixture of 180 ml of 6 M HCl and 200 g of crushed ice. After 15 minutes the precipitate was collected on a sintered-glass funnel and washed with water. The precipitate was then purified by sublimation. The crude product was placed in an inverted Petri dish which was placed on a hot plate. The plate was warmed until the top surface of the apparatus was too hot to touch. The ferrocene crystals were collected over a period of several hours.

Synthesis of Nickelocene

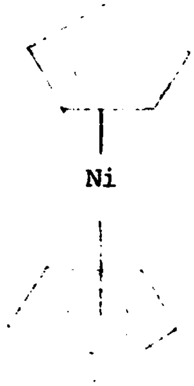

Purpose. A synthesis of nickelocene paralleling that of ferrocene was attempted in the hope of finding a simple, mild-conditioned, and easily reproducible synthesis. The synthesis of nickelocene was also to provide additional experience in inorganic synthesis techniques.

Procedure. $NiBr_2$ was made using the synthesis in Eisch and King[3] in 0.1 of the amounts recommended. The reaction was carried out in a 500 ml three-necked flask fitted with a magnetic stirring bar, reflux column with drying tube, a pressure-equalizing dropping funnel, and a nitrogen inlet. 150 ml of 1,2-dimethoxyethane was placed in the flask along with 3 g of nickel powder. Nitrogen was admitted and 2.5 ml of bromine were added dropwise. The resulting precipitate, $NiBr_2$, was kept in the 1,2-dimethoxyethane and was used in place of the $FeSO_4$/DMSO used in the synthesis of ferrocene. The overall reaction was:

$$8KOH + 2C_5H_6 + NiBr_2 \text{---}> Ni(C_5H_5)_2 + 2KBr + 6KOH + 2OH_2O$$

Rather than pouring the resulting solution into ice, the solution was filtered under nitrogen. The filtrate was then evaporated to dryness on a rota-vap using a dry-ice/acetone trap and a roughing pump. The residue was then refluxed with hexane which had been dried with calcium hydride. The attempt to extract the nickelocene with hexane was unsuccessful. The residue was then refluxed with dichloromethane.

Results and Discussion. The reaction producing $NiBr_2$ was run in excess nickel and went virtually to completion. The magnetic stirring bar provided an excellent means of removing the excess nickel. However, the reaction took longer than if the recommended stirring motor had been used because when stuck to the stirring bar the nickel offers less surface area since the inner layers are protected. As the reaction progressed the outer layers of $NiBr_2$ fell off allowing the reaction to continue.

Nickelocene is much more sensitive to air than ferrocene, the pure crystals oxidizing over several days but oxidizing quickly in solution. The DMSO used as a solvent for the $FeSO_4 \cdot 7H_2O$ contained too much water to be used in the synthesis of nickelocene. However, the formation of $NiBr_2$ could be carried out in 1,2-dimethyoxyethane, the same solvent used for the synthesis of ferrocene. Additionally, KOH serves as a good drying agent for 1,2-dimethoxyethane. It was expected that the synthesis of nickelocene would proceed in much the same manner as that of ferrocene. However, the behavior of the resulting residue which was not soluble in hexane or dichloromethane although nickelocene is indicates the desired product was not formed. The infrared spectrum shows only the presence of C-H and C=C bonds. It is not similar to that of ferrocene as would be expected. It is possible that a reduced form of nickelocene was made but there is no real indication of this. Also, such a compound would be unstable in air. Apparently some type of complex(es) was formed, but the nature of this complex is unknown.

Another Synthesis of Nickelocene

Purpose. The purpose of this procedure was to synthesize nickelocene and perhaps to provide insight into why the previous synthesis did not work.

Procedure. The procedure in Eisch and King was used with 0.1 the amount of reactants. The reactions involved are shown below.

$$Ni + Br_2 \dashrightarrow NiBr_2$$

$$NiBr_2 + 2(C_2H_5)_2NH + 2C_5H_6 \dashrightarrow (C_5H_5)_2Ni + 2[(C_2H_5)_2NH_2]Br$$

$NiBr_2$ was prepared as before. The solvent was evaporated and nitrogen was admitted. 100 ml of diethylamine were added. 10 ml of cyclopentadiene were then added dropwise. After stirring overnight the solvent was removed on a rota-vap. The flask was flushed with nitrogen and the residue was transferred to the thimble of a Soxhlet extraction apparatus. A continuous extraction with boiling hexane was carried out for about 3 hours. The hexane was allowed to cool and the volume was reduced to start crystallization.

Data and Observations.

- Excess nickel was used but some red color remained indicating the presence of bromine.
- A blue solution resulted from the addition of diethylamine to $NiBr_2$.
- The solution turned green with the addition of cyclopentadiene.
- As evaporation on the rota-vap proceeded the residue turned from green to dark red-brown. A large amount of residue was left.
- The extract with hexane was also red-brown.
- Crystals formed on the edge of the flask with the reduction in volume. Some small green crystals were seen.
- Evaporation to dryness left many more crystals.
- Sublimation using a cold-finger and roughing pump at room temperature provided no results.

Results and Discussion. The procedure proceeded in a textbook fashion until the diethylamine solvent was evaporated on a rota-vap. Apparently the vacuum was not good, allowing the residue to oxidize on contact with air. The resulting residue was a combination of diethylammonium chloride and nickelocene. The nickelocene was most likely a mixture of nickelocene, oxidized nickelocene, and the salt nickelocene bromide.

The extraction with hexane should have left most of the diethylammonium chloride behind. The reduction in volume did not produce crystallization because the product oiled out in the hexane. However, crystals formed along the edge of the solvent in the flask. The small green crystals were nickelocene. The remaining red-brown crystals are probably nickelocene bromide. It should be possible with further work to isolate nickelocene through sublimation under different conditions, a different solvent for extraction, or selective crystallization by replacing bromine with a larger anion. A good yield of $(C_5H_5)_2Ni^+Br^-$ was obtained by counter solvent crystallization using CH_2Cl_2/hexane.

Synthesis of the Ferracobaltocene $C_5H_5CoC_4H_4Fe(CO)_3$

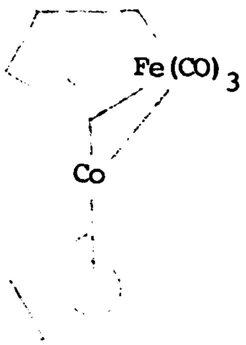

Purpose. $C_5H_5CoC_4H_4Fe(CO)_3$ is one of the compounds in the *isostructural series of compounds* which it is the goal of this project to synthesize and study. This compound was chosen to be synthesized first since it has already been made by other researchers.

Procedure. (Tricarbonylferracyclopentadiene) cyclopentadienylcobalt or ferracobaltocene has been synthesized by King, Holt, Radnia, and McKennis[4] with the following reaction:

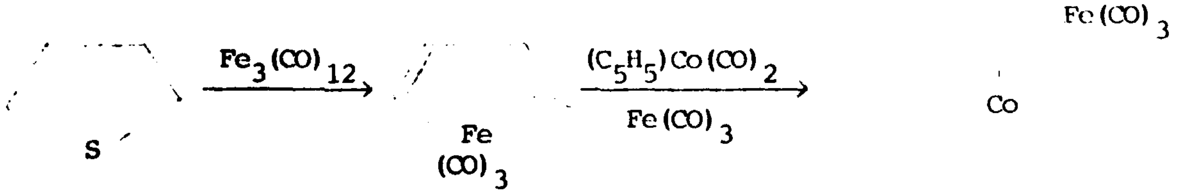

The reaction was performed under nitrogen with a reported yield of 17%. From the crystal structure it is known that the ring is nearly planar and all bonds have double bond character, indicating aromaticity. NMR shows the different environments of the H's due to the bridging carbonyl. This carbonyl is placed asymmetrically between the two irons.

The reaction was run in a three-necked flask equipped with a Soxhlet extractor and reflux column and with a nitrogen inlet. 6 g of $Fe_3(CO)_{12}$ were added to the thimble of the Soxhlet extraction apparatus. 2.5 ml of thiophene were added to the flask along with 250 ml of n-heptane. The extraction proceeded until only a faint green color remained in the solvent surrounding the thimble. The heptane was then evaporated with a rota-vap and roughing pump with a dry-ice/acetone trap. The resulting residue was sublimed at 45°C with a cold-finger and roughing pump. The residue was tested for solubility.

<u>Data and Observations</u>.

- $Fe_3(CO)_{12}$ was dark green and clumped together due to the rapid absorption of some water from the air.
- As the reaction proceeded a shiny black mirror surface covered the flask.
- The residue consisted of a black material which stuck to the magnetic stirring bar and of a very shiny "silver" mirror surface on the bottom of the flask.
- The sublimation was unsuccessful, but a few small black crystals formed.
- The residue could be pressed into fairly large shiny, flat black sheets.
- The residue was insoluble in acetone, CH_2Cl_2, water, DMSO, concentrated sulfuric acid, and strong NaOH. Soaking overnight in chromerge allowed the residue to be scrubbed out but it did not appear to dissolve.

Results and Discussion. Additional n-heptane was used due to the volume of the Soxhlet. It was not desirable to have the flask run dry. The trap was necessary in the evaporation because of the poisonous by-product $Fe(CO)_5$ which was given off. The desired product was obviously not obtained. The sublimation failed. The IR of unreacted $Fe_3(CO)_{12}$ shows the presence of carbonyls in a quite large band. The carbonyl stretch is missing from the spectrum of the residue. The residue contains iron since it is very magnetic. The lack of solubility is puzzling. FeS, a black solid, was an expected by-product. From the lack of carbonyls it can be assumed that the product, if it had formed, decomposed. It is most likely that the reaction conditions in boiling heptane were too harsh, blowing the compound apart. CO was lost leaving behind iron and sulfur. Undoubtedly a mixture of different iron-sulfur complexes formed. Some of the complexes were probably quite large, helping to explain the lack of solubility.

Modified Synthesis of $C_4H_4Fe_2(CO)_6$

Purpose. The purpose of this synthesis was to obtain $C_4H_4Fe_2(CO)_6$ for use in the synthesis of ferracobaltocene. It was hoped that milder reaction conditions would prevent the product from being blown apart.

Procedure. A simple reflux of 1 g $Fe_3(CO)_{12}$ with 1 ml thiophene in 250 ml of CH_2Cl_2 was performed. A similar reflux was performed in hexane.

Results and Discussion. The Soxhlet extraction had been used in the original procedure due to the limited solubility of $Fe_3(CO)_{12}$ in heptane. Since it is much more soluble in CH_2Cl_2 and hexane, it was added directly to the thiophene mixture. Neither solvent provided a successful synthesis. As the reaction proceeds the frequency of carbonyl stretching is expected to change because of the various environments of the carbonyls in $C_4H_4Fe_2(CO)_6$. The IR of $Fe_3(CO)_{12}$ and thiophene in CH_2Cl_2 shows no difference in the frequency of carbonyl stretching from that of unreacted $Fe_3(CO)_{12}$. Additionally, no change could be seen in the reaction flask after refluxing. FeS had been expected as a by-product. The spectra of $Fe_3(CO)_{12}$ and thiophene in hexane and with $FeCl_3$ do not differ from the spectrum of $Fe_3(CO)_{12}$ in hexane, again indicating no reaction. $FeCl_3$ had been added in an attempt to force the reaction to go.

CONCLUSIONS AND RECOMMENDATIONS

The synthesis of ferrocene was successful and provided excellent experience in inorganic synthesis techniques. The synthesis of nickelocene paralleling that of ferrocene was unsuccessful. The reason for this failure is unclear but may have been due to the harsher reducing condition in which the reaction was carried out when compared to the textbook synthesis. The product was apparently some type of nickel complex. The textbook synthesis worked well but the addition of air due to a poor vacuum on the rota-vap and the presence of bromine produced a mixture of nickelocene and nickelocene bromide. With some additional work nickelocene may be isolated. This second synthesis is a good procedure to use, especially in the synthesis of fairly large quantities of nickelocene for laboratory use.

Little progress was made toward the goal of this project -- the synthesis and characterization of the isostructural series of metallametallocenes. Although ferracobaltocene has been synthesized, the reaction proved irreproducible because the initial step in the reaction could not be performed successfully. Although the results of Dettlaf and Weiss were not reproduced, this synthesis offers more promise than the ones in the dichloromethane or hexane solutions. I believe the first failure may have been due to running the extraction too long, allowing the product to decompose. Another possibility is that at this altitude heptane boils at a lower temperature. If the reaction is sensitive to temperature, a high enough temperature may not have been achieved. The reaction would not proceed as expected and less energetic pathways to various iron-sulfur complexes were pursued. If this was the case, extraction with octane or some other solvent which at this altitude boils near the sea-level boiling point of heptane may provide successful results. Once ferracobaltocene is synthesized, parallel syntheses should be possible for ferraferrocene and ferranickelocene, although reducing and oxidizing mediums may be required.

Once the isostructural series is formed there are a number of areas of interest to investigate. Depending on the ease of adding and removing ligands on the iron, the compounds may have catalytic uses. In order to determine this the electronic structures of these compounds must be determined. Variation in the electron density around the metal center could be determined using cyclic voltammetry. One would expect this to vary across the series. The degree of variation would provide a measure of just how great the sharing along the metal-metal bond is. Likewise the effect on carbonyl stretching frequencies should be examined using infrared spectroscopy. The frequencies should vary as back-donation varies as a result of the interaction between the two metals. The greater the donation by the sandwich metal to the iron the less back-donation expected. The differences in the electronic environment of the iron and the sandwich metal may be examined using both cyclic voltammetry and Mossbauer spectrometry. Mossbauer spectrometry may also be used to examine the oxidation potentials of the sandwich metals. Lastly, ring distortion may be examined using ^{1}H-NMR and crystal structure. A spectrum similar to that of $C_4H_4Fe_2(CO)_6$ would indicate some distortion. From the C-C bond distances the degree of aromaticity could be determined. This may vary across the series. These areas of investigation should help characterize the electronic structures of the compounds and offer an indication of possible catalytic ability.

In conclusion, it is possible to synthesize the metallametallocene $C_5H_5CoC_4H_4Fe(CO)_3$. The isostructural species of ferraferrocene and ferranickelocene should also prove possible to synthesize. In their most stable forms these compounds will likely exist as anions and cations.

References

1. F.A. Cotton and G. Wilkinson, Advanced Inorganic Chemistry, 4th Ed., John Wiley & Sons, 1980, p. 63.

2. W. Jolly, The Synthesis and Characterization of Inorganic Compounds, Prentice-Hall, Inc., 1970, p. 484.

3. Eisch and King, Organometallic Synthesis, Vol. I, Academic Press, 1965, p. 72.

4. M. King, E.M. Holt, P. Radmia, and J.S. McKennis, Organomet; 1 1982, 1718-1720.

5. G. Dettlaf and E.O. Weiss, J. Organomet. Chem., 108, 1976, 213.

Chapter 8

A STUDY OF THE PIGMENTS ISOLATED FROM THE PINK ROOT FUNGUS, PYRENOCHAETA TERRESTRIS

by Henry H. Shin and James R. Wright

ABSTRACT

Pyrenochaeta terrestris (Hansen), Gorenz, J.C. Walker, and Larson is the casual organism of the pink root of onions. To the chemist this pink color is of interest. Numerous attempts have been made to determine the compound and/or compounds responsible for this red to pink coloration of the fungus. This study was another attempt to isolate the pigment compounds and to determine what factors affect the pigment production.

The fungus was grown using two different media, a sucrose or starch salts solution. The starch solution gave a greater pink to red coloration. Using thin layer chromatography (TLC), five pigment materials appear to have been isolated from the mycelium of *Pyrenochaeta terrestris* grown on a sucrose salts solution medium. Attempts to identify these pigments have not been successful.

TITLE: A Study of the Pigments Isolated from the Pink Root Fungus, *Pyrenochaeta Terrestris*, Henry H. Shin and J.R. Wright, Department of Chemistry, USAF Academy, Colorado Springs, Colorado 80840.

INTRODUCTION

The pink root of onion is a limiting factor in the production of onions in many areas of the world. This disease may affect the plant at any time during its growth period. The cause of the disease is a fungus named *Pyrenochaeta terrestris* (Hansen) Gorenz, J.C. Walker and Larson. The pink root organism is soil borne and attacks the roots of onion, in which a pink color is produced.

Taubenhaus, *et. al*. (1) first observed this disease and reported that affected bulbs remained small and undersized and therefore were unsatisfactory for market. The fungal organism was observed in 1926 by Hansen (2,3,4), who identified it as *Phoma terrestris* (Hansen). Later in 1948 this organism was reclassified as *Pyrenochaeta terrestris* by Gorenz, J.C. Walker and Larson (5). The structure of the fungus and host tissue has been described by Kreutzer (6) and Struckmeyer, *et. al*. (7).

Planting resistant varieties of onions seems to be the only method of control. There is no practical way to erradicate the fungus from infected soil.

To the chemist this pink discoloration of the roots of the diseased plant has attracted interest. Attempts have been made to determine what compound and/or compounds are responsible for this red to pink coloration. In addition pathologists would like to know if these pigments or other metabolic by-products play a role in disease expression. Also a complete study of the biosynthesis of these pigments as well as their biological significance would add greatly to the basic knowledge of science.

PREVIOUS WORK

Kreutzer (8,9) was the first worker to study the pigment of *P. terrestris*. A few years later, Kogl and Sparenburg (10) obtained a pigment, phomazarin, $C_{19}H_{17}O_8N$ from the mycelium of this fungus. The pigment was a derivative of the heterocyclic ring system azanthracene and was allocated an azanthraquinone structure with the substituents (n-butyl), $(-OH)_3$), $(-OCH_3)$, and (-COOH). Further work by Kogl, *et. al.* (11,12) led to the suggestion of two alternative structures (I or II).

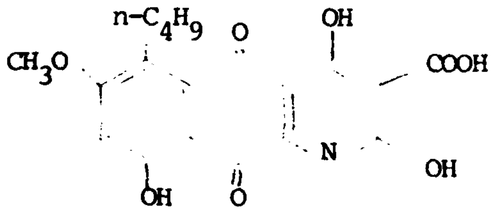

(I)

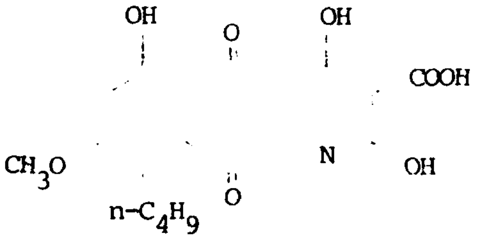

(II)

In 1960, Wright and Schofield (13) re-examined a culture of *P. terrestris* obtained from the Central Bureau vor Schimmelcultures (Baarn) and grown exactly as described in Kogl. There was isolated from the mycelium by simple extraction processes an anthraquinone compound called cynodontin (III). They were unable to isolate any compound resembling phomazarin, although they mentioned the presence of at least one other pigment.

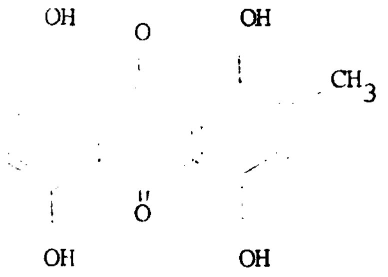

Cynodontin (III)

Birch, et. al. (14), however, found that cultures from the same source produced the pigment, phomazarin, which agree in physical properties with those described by Kogl. For reasons which they were unable to determine, the same organism grown under the usual conditions does not invariably produce this pigment. Like Wright and Schofield they observed cynodontin.

Preliminary work on the biosynthesis of phomazarin by Birch, et. al. (14) indicated that eight acetate units are involved together with a grouping arising possibly from glycine or another amino acid. The distribution of activity and spectral evidence supported structure (I) rather than (II).

Birch, et. al. (15) finally in 1979 completed structure investigations on phomazarin and have shown it to be (IV).

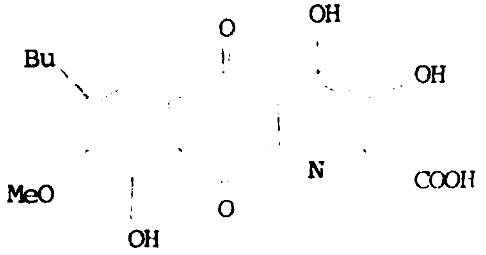

Phomazarin (IV)

Effenberger and Simpson (16) reported the same year isolation of a small amount of pigment they termed isophomazarin (V).

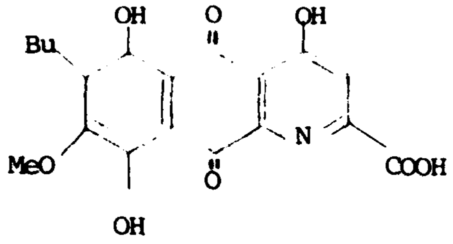

Isophomazarin (V)

Five additional metabolites have also been isolated and identified from the mycelium of Pyrenochaeta terrestris (17,18).

These compounds have been called secalonic acids A, E, G, emodin, and endocrocin. Their structures are given below (VI - X).

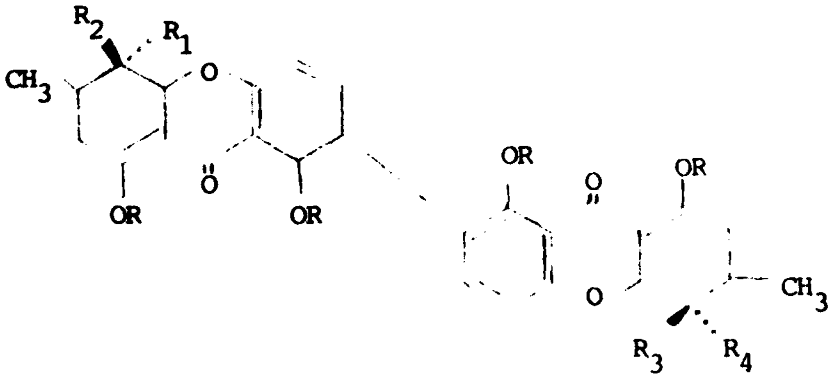

Secalonic Acid A - - - R = R_2 = R_3 = -H; R_1 = R_4 = -OH

Secalonic Acid E - - - R = R_1 = R_4 = -H; R_2 = R_3 = -OH

Secalonic Acid G - - - R = R_1 = R_3 = -H; R_2 = R_4 = -OH

(VI - VIII)

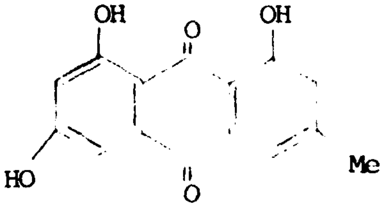

Emodin (IX)

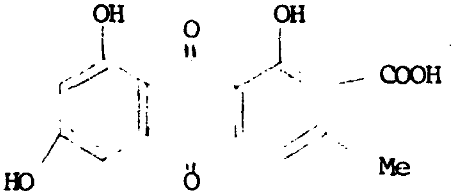

Endocrin (X)

A summary of the pigments and properties is given in Table I.

Table I. Pigments isolated from Pyrenochaeta terrestris.

Pigments	Colors	MP (°C)	Reference
Cyndontin	red	260	13
Phomazarin	orange	196	15
Isophomazarin	deep red needles	215-216	16
Secalonic acid A	orange needles	208-209	17
Secalonic acid E	yellow	206-208	17
Secalonic acid G	yellow	206-207	17
Emodin	orange plates	257-259	18
Endocrin	reddish-orange	289-314	18

OBJECTIVES

(1) To isolate and identify completely all the pigment materials associated with this fungus (examine the large amount of purple gum).

(2) To determine reasons why P. terrestris produces the pigment phomazarin in some instances and cynodontin at other times.

(3) To see if using different media would have any effect on pigment production.

PROCEDURES

The procedures are divided into two sections. The first section will deal with the procedures followed to grow mycelium while the second section will deal with the procedures used to isolate the pigments.

Growth of the fungus. - An isolate of Pyrenochaeta terrestris (designated as P.t.) was obtained from the American Type Culture Collection, Bethesda, Maryland. Stock cultures were carried on potato dextrose agar and transferred at regular intervals. Thirty grams of sucrose was added to the following basal medium for growth of the fungus. The basal medium was of the following composition: $MgSO_4 \cdot 7H_2O$ - 0.5 g; KH_2PO_4 - 1.5 g; $NaNO_3$ - 1.0 g; 0.5 ml of a $Fe(NO_3)_3$ solution; 0.5 ml of a minor elements solution; and distilled water added to make a final volume of 1 liter. The ferric nitrate solution and minor elements solution were of such concentration that the final concentrations in a liter of medium were as follows: Fe - 0.2 mg; Cu and Zn - 0.1 mg; and Mo and Mn - 0.02 mg. Mn, Cu, and Zn were added as the sulfates and Mo as sodium molybdate. The medium was adjusted to pH 4.5 using 10 per cent sodium hydroxide and dispensed 25 ml/125 ml Erlenmeyer flask. The flasks were plugged with cotton and autoclaved 15 minutes at 1.05 kg/cm^2 pressure. The chemicals used were chemically pure quality obtained from commercial sources. Inoculum was prepared by transferring small mycelial biscuits from a culture growing on potato dextrose agar into several flasks of medium. The flasks were shaken gently and set aside for growth at room temperature. After 6-8 days, mycelial growth was visible. The content of these flasks were ground for 1 minute with a Waring blender and 1 ml of the suspension was pipetted into each of the test flasks. All procedures were carried out aseptically. The flasks were incubated at room temperature (25-28°C). After 21 days, the mycelial mats were harvested by filtration using cheese cloth, washed with distilled water, and then dried in 110°C oven for 24 hours. The mycelium from the starch solution was grown the same way except instead of sucrose and basal medium, a starch solution was used. The solution was composed of 50 g starch, 1 g potassium dihydrogen phosphate, 0.5 g calcium chloride and 0.001 g of ferrous sulfate heptahydrate in 1 liter of distilled water.

Extraction of mycelium. - Known quantities of dried mycelium were finely powdered using a mortar and pestle and then exhaustively extracted using a Soxhlet apparatus. The mycelium was extracted first with diethylether, acetone and then methanol. The residual mycelium was washed using 20 ml of petroleum ether. It was then air dried and acidified with 35 ml of 2 M aqueous HCl. The mycelium was repeatedly washed with water until neutral. Then the mycelium was further extracted with diethylether, chloroform and acetone. Solids from the above extracts were obtained by blowing a small stream of air over the flasks containing the solvents or by using a vacuum rotary film evaporator at a temperature no greater than 40°C. Attempts were made to recrystallize the solids from the first set of extractions (ether, acetone, and methanol) using pyridine. On the solids from the second extraction with chloroform, a mass spectra was performed using the mass spectra instrument of the Frank J. Seiler Research Laboratory. Analysis was performed by Mr. Lloyd Pflug. The solids from the chloroform extraction were next separated using preparatory silica gel thin layer chromatography.

Elution was performed with hexane, ethylacetate - (50/50,v/v) and ethylacetate - hexane (30/70, v/v). The eluant ratio of 50/50, v/v of ethylacetate - hexane gave the best results. After air drying, the different pigments were identified visually and by using a short and long wave length UV mineral light. The different pigment areas were cut from the silica gel and extracted with ethylacetate. The pigments were further isolated by filtration and evaporated of the solvent using a vacuum rotary film evaporator.

RESULTS AND OBSERVATIONS: The following results and observations are noted and given in the tables below.

Table II. First extraction of the dried mycelium of *Pyrenochaeta terrestris*.

Solvents	Solutions	Crystals	Recrystallizing solvents	Solids
Ether	dark pink	red	pyridine	red/ purple
Acetone	red/orange	red	pyridine	red/ purple
Methanol	dark red	red	pyridine	red purple

Table III. Second extraction of the dried mycelium of *Pyrenochaeta terrestris*.

Solvents	Solutions	Crystals	Recrystallization solvents	Solids
Ether	dark orange	red/orange	pyridine	red/ orange
Chloroform	orange-yellow	red/orange	chloroform	red/ orange
Acetone	deep red	red/orange	-	-

Table IV. Diagram and comments about the thin layer chromatography of the chloroform extract of Pyrenochaeta terrestris. Ethylacetate - hexane (50/50,v/v) was used to develop the TLC plates.

TLC Plate

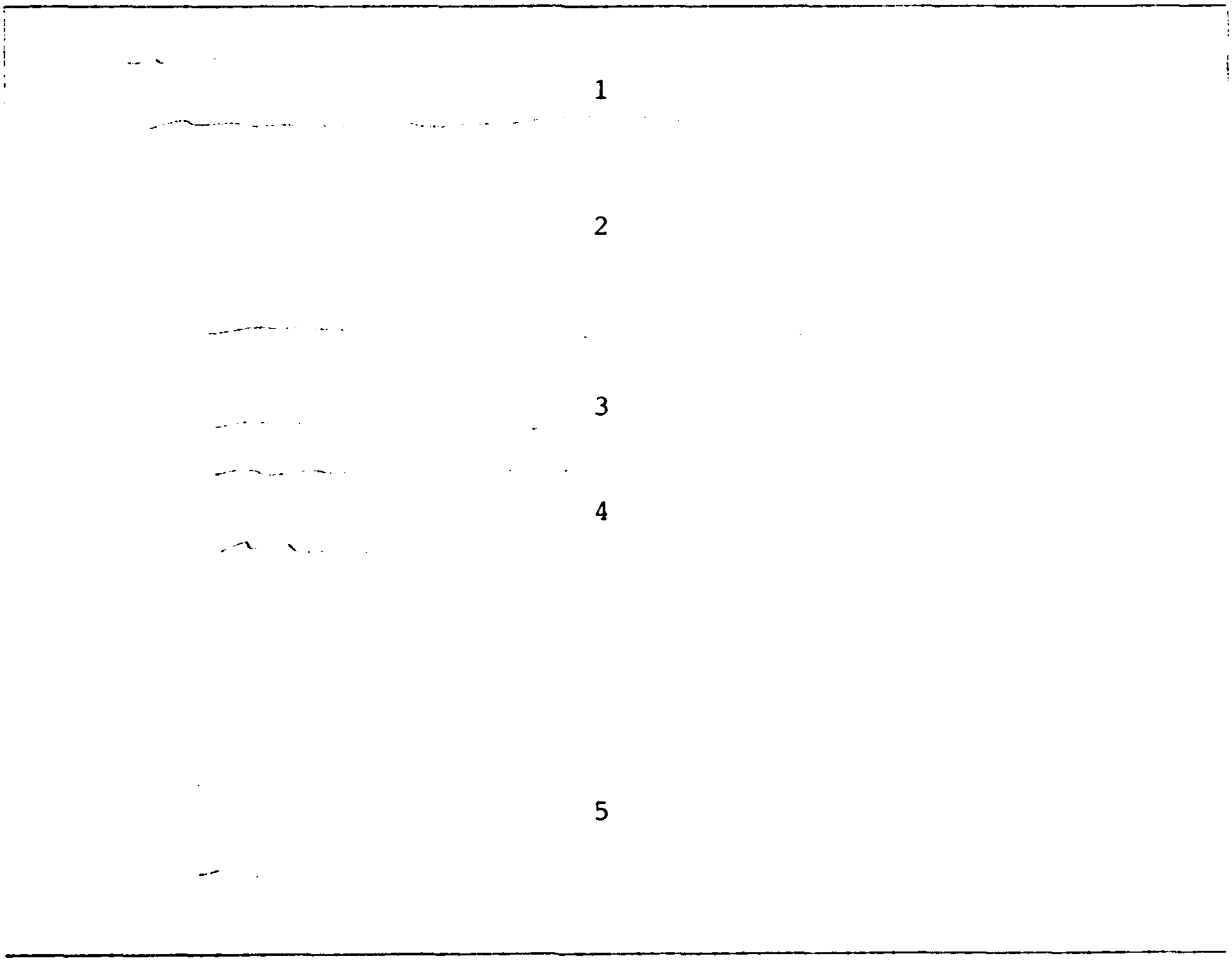

Wavelengths used	Ethyl Acetate Solution	Compound	Silica Gel	No.
short	yellow	oily yellow	white	1
short, long	dark pink	pink solid	white	2

long	pink	pink solid	white	3
long	yellow	yellow solid	white	4
long	purple-red	oily yellow	pink	5

The oily compounds might indicate a mixture of different pigments. As for silica gel #5, the pink color indicated an unisolated pigment, where as white colors indicated that the pigments were separated from the silica gel. Due to lack of time attempts to further isolate the pink pigment from the silica gel strip #5 could not be performed.

Table V. Mass Spectrum of Chloroform Extract:

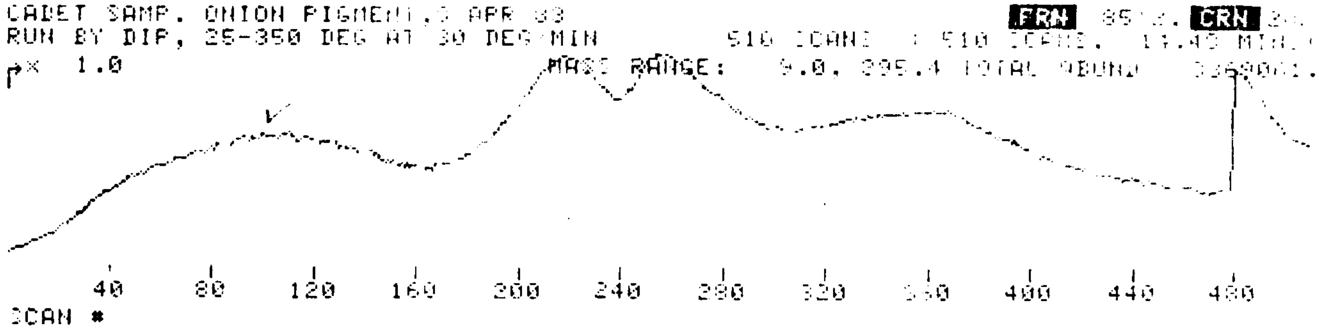

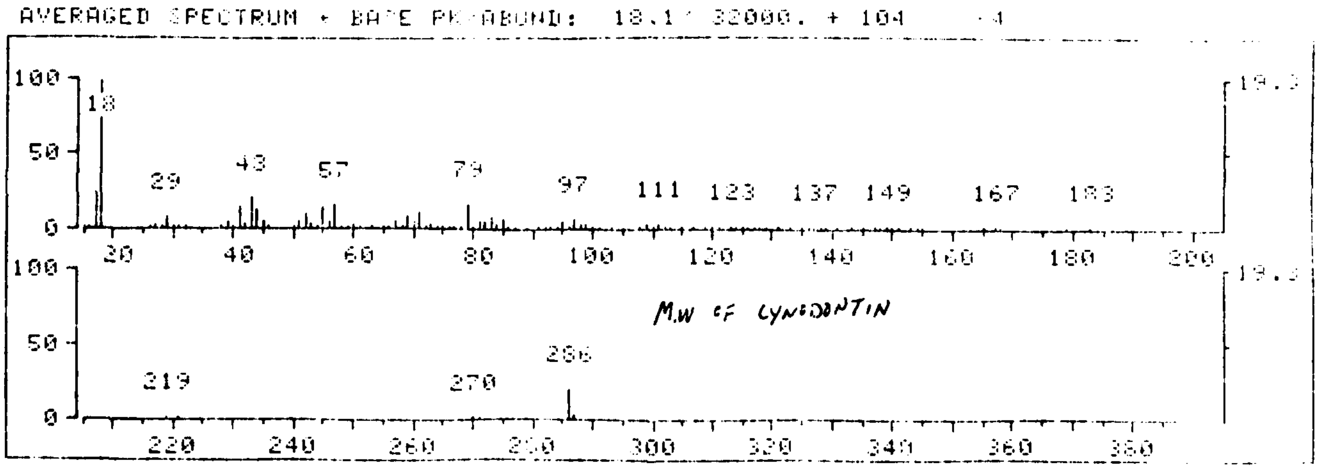

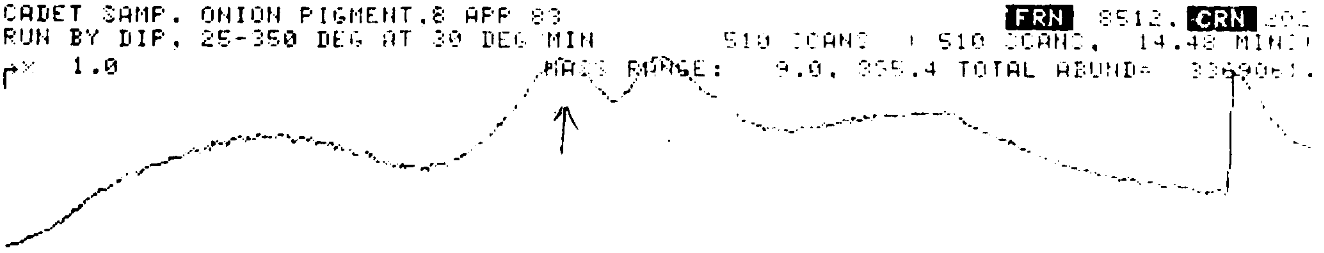

The mass spectrum done on the chloroform extract indicated a molecular weight of 286 which is the molecular weight of cynodontin. The sole purpose of doing a mass spectrum at that time was to see if cynodontin might be present in the chloroform extract.

Growth of Mycelium

The colors of the mycelial mats were definitely different between the mycelium grown in sucrose solution and the mycelium grown in starch solution. The dried mycelium of starch source was very pink whereas the dried mycelium of sucrose source was brownish/green. According to the literature the mycelium with the higher proportion of cyndontin would have a pink color while the mycelium with a large amount of secalonic acids and cynodontin would have a brownish green color (18).

CONCLUSIONS. From the above observations it appears that at least five compounds can be isolated. Attempts to identify these compounds have not been successful. It appears visually that the starch solution favors the production of red pigments whereas the sucrose solution if favorable to the formation of other compounds. More additional work is needed to isolate and completely identify the pigments from the fungus, *Pyrenochaeta terrestris*.

RECOMMENDATIONS. The following recommendations are made by C1C Henry H. Shin who performed the cited work as his independent research study for chemistry 499.

1. Take pictures of research to document the work performed. These could be used as part of a presentation for the American Chemical Society Meeting in Miniature.

2. Start work in the laboratory much earlier. Two semesters of Independent Study would have given some positive results.

3. Try to identify the pigment already isolated using the tools of the organic chemist.

4. Use thin layer chromatography to separate and isolate the pigments.

5. Quantify the amounts of the pigments present in the mycelium grown using different cultural media.

REFERENCES CITED:

1. J.J. Taubenhaus and A.D. Johnson, Phytopathology, 7, 59 (1917).

2. H.N. Hansen, Science, 64, 525 (1926).

3. H.N. Hansen, Phytopathology, 19, 691 (1929).

4. H.N. Hansen, Phytopathology, 19, 1135 (1929).

5. A.M. Gorenz, A.C. Walker, and R.H. Larson, Phytopathology, 38, 381 (1948).

6. W.A. Kreutzer, Phytopathology, 31, 907 (1941).

7. B.E. Struckmeyer, C.G. Nichols, R.H. Larson, and W.H. Gabelman, Phytopathology, 52, 1163 (1962).

8. W.A. Kreutzer, Phytopathology, 29, 629 (1939).

9. W.A. Kreutzer, J. Colorado Wyoming Acad. Sci., 89, 3680 (1940).

10. F. Kogl and J. Sparenburg, Rec. trav. chim., 59, 1180 (1940).

11. F. Kogl and F.S. Quackenbush, Rec. trav. chim., 63, 251 (1944).

12. F. Kogl and G.C. van Wessem, and O.I. Elsbach, Rec. trav. chim., 64, 23 (1947).

13. D.E. Wright and K. Schofield, Nature, 188, 233 (1960).

14. A.J. Birch, R.I. Fryer, P.J. Thompson, and H. Smith, Nature, 190, 441 (1961).

15. A.J. Birch, D.N. Butler, R. Effenberger, R.W. Richard and T.J. Simpson, J. Chem. Soc. Perkin Trans I, 3, 807 (1979).

16. R. Effenberger and T.J. Simpson, J. Chem. Sec. Perkin Trans I, 3, 823 (1979).

17. C.C. Howard and R.A.W. Johnstone, J. Chem. Soc. Perkin Trans I, 20, 2440 (1973).

18. I. Kurobane, L.C. Vining and A.G. McInnes, J. Antibiot (Tokyo), 32, 1256 (1979).